

# Extended Studies of Separability Functions and Probabilities and the Relevance of Dyson Indices

Paul B. Slater\*

*ISBER, University of California,  
Santa Barbara, CA 93106*

(Dated: December 11, 2021)

## Abstract

We report substantial progress in the study of *separability functions* and their application to the computation of *separability probabilities* for the real, complex and quaternionic qubit-qubit and qubit-qutrit systems. We expand our recent work (*J. Phys. A* **39**, 913 [2006]), in which the Dyson indices of random matrix theory played an essential role, to include the use of not only the volume element of the Hilbert-Schmidt (HS) metric, but also that of the Bures (minimal monotone) metric as measures over these finite-dimensional quantum systems. Further, we now employ the Euler-angle parameterization of density matrices ( $\rho$ ), in addition to the Bloore parameterization. The Euler-angle separability function for the minimally degenerate complex two-qubit states is well-fitted by the sixth-power of the participation ratio,  $R(\rho) = \frac{1}{\text{Tr}\rho^2}$ . Additionally, replacing  $R(\rho)$  by a simple linear transformation of the Verstraete-Audenaert-De Moor function (*Phys. Rev. A*, **64**, 012316 [2001]), we find close adherence to Dyson-index behavior for the real and complex (nondegenerate) two-qubit scenarios. Several of the analyses reported help to fortify our conjectures that the HS and Bures separability probabilities of the complex two-qubit states are  $\frac{8}{33} \approx 0.242424$  and  $\frac{1680(\sqrt{2}-1)}{\pi^8} \approx 0.733389$ , respectively. Employing certain *regularized beta functions* in the role of Euler-angle separability functions, we closely reproduce—consistently with the Dyson-index *ansatz*—several HS two-qubit separability probability conjectures.

**Mathematics Subject Classification (2000):** 81P05; 52A38; 15A90; 28A75

PACS numbers: Valid PACS 03.67.-a, 02.30.Cj, 02.40.Ky, 02.40.Ft

---

\*Electronic address: slater@kitp.ucsb.edu

## Contents

<b>I. Introduction</b>	3
A. Bloore parameterization of density matrices	4
B. Euler-angle parameterization of density matrices	5
C. Immediately preceding studies	6
D. Objectives	6
<b>II. Bloore-parameterization separability functions</b>	7
A. Quaternionic two-qubit Hilbert-Schmidt analysis	7
1. Estimated separability function and probability	8
2. Supplementary estimation of $R_1$ constant	11
3. Conjectured complex and quaternionic separability functions and probabilities	12
B. <i>Truncated</i> quaternionic analysis ( $\beta = 3$ )	12
C. Real and complex Qubit- <i>Qutrit</i> Hilbert-Schmidt Analyses	14
1. Relations to previous qubit-qutrit analyses [11, 17]	20
D. Bures two-qubit separability functions and probabilities	20
1. Review of earlier parallel Hilbert-Schmidt findings	21
2. Four-parameter density-matrix scenarios	23
3. Five-parameter density-matrix scenarios	27
4. Additional analyses	29
5. Discussion	30
<b>III. Euler-angle-parameterization separability functions</b>	31
A. Complex two-qubit case	32
B. <i>Trivariate</i> separability function for <i>volume</i> computation	32
C. <i>Bivariate</i> separability function for <i>area</i> computation	35
D. Participation ratios	37
E. Verstraete-Audenaert-De Moor function	40
F. Beta function fits to Euler-angle separability functions	40
<b>IV. Summary</b>	41
<b>Acknowledgments</b>	43

## I. INTRODUCTION

For several years now, elaborating upon an idea proposed in [1], we have been pursuing the problem of deriving (hypothetically exact) formulas for the proportion of states of qubit-qubit [2] and qubit-qutrit [3] systems that are *separable* (classically-correlated) in nature [4, 5, 6, 7, 8, 9, 10, 11]. Of course, any such proportions will critically depend upon the measure that is placed upon the quantum systems. In particular, we have—in analogy to (classical) Bayesian analyses, in which the *volume element* of the *Fisher information* metric for a parameterized family of probability distributions is utilized as a measure (“Jeffreys’ prior”) [12]—principally employed the volume elements of the well-studied (Euclidean, flat) Hilbert-Schmidt (HS) and Bures (*minimal* monotone or symmetric-logarithmic-derivative [SLD]) metrics (as well as a number of other [non-minimal] *monotone* metrics [8]).

Życzkowski and Sommers [13, 14] have, using methods of random matrix theory [15] (in particular, the Laguerre ensemble), obtained formulas, general for all  $n$ , for the HS and Bures *total* volumes (and hyperareas) of  $n \times n$  (real and complex) quantum systems. Up to normalization factors, the HS total volume formulas were also found by Andai [16], in a rather different analytical framework, using a number of (spherical and beta) integral identities and positivity (Sylvester) conditions. (He also obtained formulas—general for any monotone metric [including the Bures]—for the volume of *one*-qubit [ $n = 2$ ] states [16, sec. 4].)

Additionally, Andai did specifically study the HS *quaternionic* case. He derived the HS total volume for  $n \times n$  quaternionic systems [16, p. 13646],

$$V_{quat}^{HS} = \frac{(2n-2)! \pi^{n^2-n}}{(2n^2-n-1)! \prod_{i=1}^{n-2} (2i)!}, \quad (1)$$

giving us for the two-qubit ( $n = 4$ ) case that will be our specific initial interest here, the 27-dimensional volume,

$$\frac{\pi^{12}}{7776000} \cdot \frac{1}{40518448303132800} = \frac{\pi^{12}}{315071454005160652800000} \approx 2.93352 \cdot 10^{-18}. \quad (2)$$

(In the analytical setting employed by Życzkowski and Sommers [13], this volume would appear as  $2^{12}$  times as large [16, p. 13647].)

If one then possessed a companion volume formula for the *separable* subset, one could immediately compute the HS two-qubit quaternionic separability *probability* ( $P_{quat}^{HS}$ ) by taking the ratio of the two volumes. In fact, following a convenient paradigm we have developed, and will employ several times below, in varying contexts, we will compute  $P_{quat}^{HS}$  as the product ( $R_1 R_2$ ) of two *ratios*,  $R_1$  and  $R_2$ . The first (24-dimensional) factor on the left-hand side of (2) will serve as the denominator of  $R_1$  and the second (3-dimensional) factor, as the denominator of  $R_2$ . The determinations of the *numerators* of such pairs of complementary ratios will constitute, in essence, our (initial) principal computational challenges.

### A. Bloore parameterization of density matrices

One analytical approach to the separable volume/probability question that has recently proved to be productive [17]—particularly, in the case of the Hilbert-Schmidt (HS) metric (cf. [18])—makes fundamental use of a (quite elementary) form of density matrix parameterization first proposed by Bloore [19]. This methodology can be seen to be strongly related to the very common and long-standing use of *correlation matrices* in statistics and its many fields of application [20, 21, 22]. (Correlation matrices can be obtained by standardizing *covariance* matrices. Density matrices have been viewed as covariance matrices of multivariate normal [Gaussian] distributions [23]. Covariance matrices for certain observables have been used to study the separability of finite-dimensional quantum systems [24]. The possible states of polarization of a two-photon system are describable by six Stokes parameters and a  $3 \times 3$  “polarization correlation” matrix [25].)

In the Bloore (off-diagonal scaling) parameterization, one simply represents an off-diagonal  $ij$ -entry of a density matrix  $\rho$ , as  $\rho_{ij} = \sqrt{\rho_{ii}\rho_{jj}}w_{ij}$ , where  $w_{ij}$  might be real, complex or quaternionic [26, 27, 28] in nature. The particular attraction of the Bloore scheme, in terms of the separability problem in which we are interested, is that one can (in the two-qubit case) implement the well-known Peres-Horodecki separability (positive-partial-transpose) test [29, 30] using only the ratio,

$$\mu = \sqrt{\nu} = \sqrt{\frac{\rho_{11}\rho_{44}}{\rho_{22}\rho_{33}}}, \quad (3)$$

rather than the four (three independent) diagonal entries of  $\rho$  individually [11, eq. (7)] [17, eq. (5)].

Utilizing the Bloore parameterization, we have, accordingly, been able to reduce the problem of computing the desired HS volumes of two-qubit separable states to the computations of *one*-dimensional integrals (33) over  $\mu \in [0, \infty]$ . The associated integrands are the *products* of *two* functions, one a readily determined jacobian function  $\mathcal{J}(\mu)$  (corresponding, first, to the transformation to the Bloore variables  $w_{ij}$  and, then, to  $\mu$ ) and the other, the more problematical (what we have termed) *separability function*  $\mathcal{S}^{HS}(\mu)$  [11, eqs. (8), (9)].

In the qubit-*qutrit* case [sec. II C], *two* ratios,

$$\nu_1 = \frac{\rho_{11}\rho_{55}}{\rho_{22}\rho_{44}}, \quad \nu_2 = \frac{\rho_{22}\rho_{66}}{\rho_{33}\rho_{55}}, \quad (4)$$

are required to express the separability conditions (choosing to compute the partial transpose by transposing four  $3 \times 3$  blocks, rather than nine  $2 \times 2$  blocks of the  $6 \times 6$  density matrices),, but analytically the corresponding HS separability functions also appear to be *univariate* in nature, being simply functions of either  $\nu_1$  or of  $\nu_2$  singly, or the product [17, sec. III],

$$\eta = \nu_1\nu_2 = \frac{\rho_{11}\rho_{66}}{\rho_{33}\rho_{44}}. \quad (5)$$

## B. Euler-angle parameterization of density matrices

Here, one can again divide the set of parameters into two groups, in a natural manner (that is, the diagonal and off-diagonal parameters in the Bloore framework). Now, the two sets are composed of the eigenvalues of  $\rho$  and of the Euler angles parameterizing the associated unitary matrix of eigenvectors [3, 31].

With both forms of parameterizations we have discussed, one can obtain the total volume of  $n \times n$  quantum systems as the *product* of integrals over the two complementary sets [13, 14]. But this direct approach no longer holds in terms of computing the separable volume. So, we have evolved the following general strategy [11, 17]. We integrate over the larger set (off-diagonal or Euler-angle parameters), *while* enforcing separability conditions, leaving us with *separability functions* that are functions of only the *smaller* set of parameters (diagonal entries or eigenvalues). Doing so, of course, substantially reduces the dimensionality of the problem.

We are, then, left with such separability functions and the ensuing task of appropriately integrating these functions over the remaining parameters (diagonal entries or eigenvalues), so as to obtain the requisite *separable volumes*.

### C. Immediately preceding studies

In our extensive numerical (quasi-Monte Carlo integration) investigation [11] of the 9-dimensional and 15-dimensional convex sets of real and complex  $4 \times 4$  density matrices, we had formulated ansätze for the two associated separability functions ( $\mathcal{S}_{real}^{HS}(\mu)$  and  $\mathcal{S}_{complex}^{HS}(\mu)$ ), proposing that they were proportional to certain (independent) *incomplete beta functions* [32],

$$B_{\mu^2}(a, b) = \int_0^{\mu^2} \omega^{a-1}(1 - \omega)^{b-1} d\omega, \quad (6)$$

for particular values of  $a$  and  $b$ . However, in the subsequent study [17], we were led to somewhat modify these ansätze, in light of multitudinous exact *lower-dimensional* results obtained there. Since these further results clearly manifested patterns fully consistent with the *Dyson index* (“repulsion exponent”) pattern ( $\beta = 1, 2, 4$ ) of random matrix theory [33], we proposed that, in the (full 9-dimensional) real case, the separability function was proportional to a specific incomplete beta function ( $a = \frac{1}{2}, b = 2$ ),

$$\mathcal{S}_{real}^{HS}(\mu) \propto B_{\mu^2}\left(\frac{1}{2}, 2\right) \equiv \frac{3}{4}(3 - \mu^2)\mu = \frac{3|\rho|^{\frac{1}{2}}}{4\rho_{22}\rho_{33}}(3\rho_{22}\rho_{33} - \rho_{11}\rho_{44}) \quad (7)$$

and in the complex case, proportional, not just to an independent function, but simply to the *square* of  $\mathcal{S}_{real}^{HS}(\mu)$ . (These proposals are strongly consistent [17, Fig. 4] with the numerical results generated in [11].) This chain of reasoning, then, immediately suggests the further proposition that the separability function in the *quaternionic* case is exactly proportional to the *fourth* power of that for the real case (and, obviously, the square of that for the complex case). It is that specific proposition we will, first, seek to evaluate here.

### D. Objectives

We seek below (sec. II A) to further test the validity of our Dyson-index ansatz, first advanced in [17], as well as possibly develop an enlarged perspective on the still not yet fully resolved problem of the two-qubit HS separability probabilities in all three (real, complex and quaternionic) cases. (In [17], we proposed, combining numerical and theoretical arguments—not fully rising to the level of a formal demonstration—that in the real two-qubit case, the HS separability probability is  $\frac{8}{17}$ , and in the complex two-qubit case,  $\frac{8}{33}$ .) A supplementary treatment of the *truncated* quaternionic scenario ( $\beta = 3$ ) is presented in sec. II B.

We investigate related separability-function questions in the qubit-*qutrit* framework, again making use of the Hilbert-Schmidt metric (sec. II C), and, also in the two-qubit setting, employing the Bures (minimal monotone) metric (sec. II D). Since it becomes more problematic to obtain separability functions in the Bures case, we explore—as originally proposed in [34]—the use of the  $SU(4)$  Euler-angle parameterization of Tilma, Byrd and Sudarshan [31] for similarly-minded purposes (sec. III).

## II. BLOORE-PARAMETERIZATION SEPARABILITY FUNCTIONS

### A. Quaternionic two-qubit Hilbert-Schmidt analysis

Due to the “curse of dimensionality” [35, 36], we must anticipate that for the same number of sample (“low-discrepancy” Tezuka-Faure (TF) [37, 38]) points generated in the quasi-Monte Carlo integration procedure employed in [11] and here, our numerical estimates of the quaternionic separability function will be less precise than the estimates were for the complex, and *a fortiori*, real cases. (An interesting, sophisticated alternative approach to computing the Euclidean volume of *convex* bodies involves a variant of *simulated annealing* [39] (cf. [40]), and allows one—unlike the Tezuka-Faure approach, we have so far employed—to establish confidence intervals for estimates.)

Our first extensive numerical analysis here involved the generation of sixty-four million 24-dimensional Tezuka-Faure points, all situated in the 24-dimensional unit hypercube  $[0, 1]^{24}$ . (The three independent diagonal entries of the density matrix  $\rho$ —being incorporated into the jacobian  $\mathcal{J}(\mu)$ —are irrelevant at this stage of the calculations of  $\mathcal{S}_{quat}^{HS}(\mu)$ . The 24 [off-diagonal] Bloore variables had been linearly transformed so that each ranged over the unit interval  $[0, 1]$ . The computations were done over several weeks, using compiled Mathematica code, on a MacMini workstation.)

Of the sixty-four million sample points generated, 7,583,161, approximately 12%, corresponded to possible  $4 \times 4$  quaternionic density matrices—satisfying nonnegativity requirements. For each of these feasible points, we evaluated whether or not the Peres-Horodecki positive-partial-transpose separability test was satisfied for 2,001 equally-spaced values of  $\mu \in [0, 1]$ .

Here, we encounter another computational “curse”, in addition to that already mentioned

pertaining to the high-dimensionality of our problem, and also the infeasibility of most (88%) of the sampled Tezuka-Faure points. In the standard manner [15, eq. (5.1.4)] [27, p. 495] [41, eq. (17)] [42, sec. II], making use of the Pauli matrices, we transform the  $4 \times 4$  *quaternionic* density matrices—and their partial transposes—into  $8 \times 8$  density matrices with [only] complex entries. Therefore, given a feasible 24-dimensional point, we have to check for each of the 2,001 values of  $\mu$ , an  $8 \times 8$  matrix for nonnegativity, rather than a  $4 \times 4$  one, as was done in both the real and complex two-qubit cases. In all three of these cases, we found that it would be incorrect to simply assume—which would, of course, speed computations—that if the separability test is passed for a certain  $\mu_0$ , it will also be passed for all  $\mu$  lying between  $\mu_0$  and 1. This phenomenon reflects the intricate (quartic *both* in  $\mu$  and in the Bloore variables  $w_{ij}$ 's, in the real and complex cases) nature of the polynomial separability constraints [11, eq. (7)] [17, eq. (5)].

### 1. Estimated separability function and probability

In Fig. 1 we show the estimate we, thus, were able to obtain of the two-qubit quaternionic separability function  $\mathcal{S}_{quat}^{HS}(\mu)$ , in its normalized form. (Around  $\mu = 1$ , one must have the evident symmetrical relation  $\mathcal{S}^{HS}(\mu) = \mathcal{S}^{HS}(\frac{1}{\mu})$ .) Accompanying our estimate in the plot is the (well-fitting) hypothetical true form (according with our Dyson-index ansatz [17]) of the HS two-qubit separability function, that is, the *fourth* power,  $\left(\frac{1}{2}(3 - \mu^2)\mu\right)^4$ , of the normalized form of  $\mathcal{S}_{real}^{HS}(\mu)$ .

For the specific, important value of  $\mu = 1$ —implying that  $\rho_{11}\rho_{44} = \rho_{22}\rho_{33}$ —the ratio ( $R_1$ ) of the 24-dimensional HS measure ( $m_{sep} = R_1^{numer}$ ) assigned in our estimation procedure to separable density matrices to the (known) total 24-dimensional HS measure ( $m_{tot} = R_1^{denom}$ ) allotted to all (separable and nonseparable) density matrices is  $R_1 = 0.123328$ . The exact value of  $m_{sep}$  is, of course, to begin here, unknown, being a principal desideratum of our investigation. On the other hand, we can directly deduce that  $m_{tot} = R_1^{denom} = \frac{\pi^{12}}{7776000} \approx 0.118862$ —our sample estimate being 0.115845—by dividing the two-qubit HS quaternionic 27-dimensional volume (2) obtained by Andai [16] by

$$R_2^{denom} = 2 \int_0^1 \mathcal{J}_{quat}(\mu) d\mu = \frac{\Gamma\left(\frac{3\beta}{2} + 1\right)^4}{\Gamma(6\beta + 4)} = \frac{1}{40518448303132800} \approx 2.46801 \cdot 10^{-17}, \quad \beta = 4. \quad (8)$$

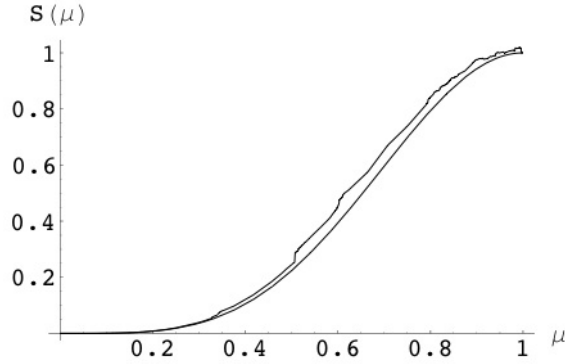


FIG. 1: Estimate—based on 64,000,000 sampled 24-dimensional points—of the normalized form of the two-qubit *quaternionic* separability function  $S_{quat}^{HS}(\mu)$ , along with its (well-fitting) hypothetical true form, the *fourth* power of the normalized form of  $S_{real}^{HS}(\mu)$ , that is,  $\left(\frac{1}{2}(3 - \mu^2)\mu\right)^4$

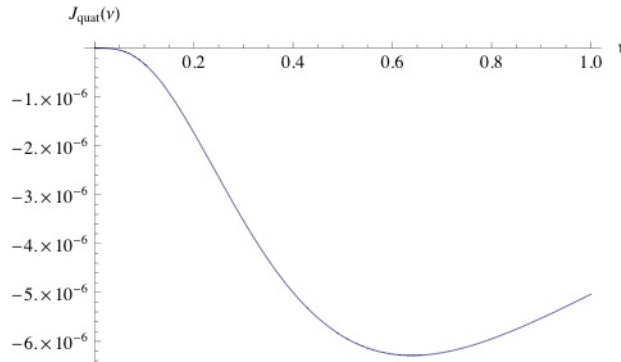


FIG. 2: The univariate quaternionic jacobian function  $\mathcal{J}_{quat}(\mu)$

Here,  $\mathcal{J}_{quat}(\mu)$  is the quaternionic jacobian function (Fig. 2), obtained by transforming the quaternionic Bloore jacobian  $\left(\rho_{11}\rho_{22}\rho_{33}(1 - \rho_{11} - \rho_{22} - \rho_{33})\right)^{\frac{3\beta}{2}}$ ,  $\beta = 4$ , to the  $\mu$  variable by replacing, say  $\rho_{33}$  by  $\mu$ , and integrating out  $\rho_{11}$  and  $\rho_{22}$ . (We had presented plots of  $\mathcal{J}_{real}(\mu)$  and  $\mathcal{J}_{complex}(\mu)$  in [11, Figs. 1, 2], and observed apparently highly oscillatory behavior in both functions in the vicinity of  $\mu = 1$ . However, a referee of [17] informed us that this was simply an artifact of using standard machine precision, and that with sufficiently enhanced precision [only recently available for plotting purposes in Mathematica 6.0]—as now employed in Fig. 2—the oscillations could be seen to be, in fact, illusory.) We theoretically can obtain the two-qubit quaternionic *separability* probability  $P_{sep/quat}^{HS}$  by multiplying the true value (which we do not beforehand know, but seek) of the ratio  $R_1$  by a second (known, computable) ratio  $R_2$ . The denominator of  $R_2$  has already been given (8). The *numerator*

of  $R_2$  is the specific value

$$R_2^{numer} = 2 \int_0^1 \mathcal{J}_{quat}(\mu) \left( \frac{1}{2}(3 - \mu^2)\mu \right)^4 d\mu = \frac{5989}{358347086242825680000} \approx 1.67128 \cdot 10^{-17}, \quad (9)$$

where, to obtain the integrand, we have multiplied (in line with our basic [Bloore-parameterization] approach to the separability probability question) the quaternionic jacobian function (Fig. 2) by the (normalized) putative form of the two-qubit quaternionic separability function. (Note the use of the  $\beta = 4$  exponent.)

The counterpart of  $R_2^{numer}$  in the 9-dimensional *real* case is  $\frac{1}{151200}$  and in the 15-dimensional *complex* case,  $\frac{71}{99891792000}$ . We further note, regarding the last denominator, that

$$99891792000 = \binom{11}{2} \frac{\Gamma(16)}{\Gamma(7)} \quad (10)$$

is the coefficient of  $\mu^2$  in  $11!L_{11}^4(\mu)$  and  $\frac{151200}{2} = 75600$  plays the exact same role in  $6!L_6^4(\mu)$ , where  $L_m^a(\mu)$  is a generalized ( $a = 4$ ) Laguerre polynomial (see sequences A062260 and A062140 in the *The On-Line Encyclopaedia of Integer Sequences*). (Also, as regards the denominator of (9),  $\frac{358347086242825680000}{3587352665} = 99891792000$ .) Życzkowski and Sommers had made use of the Laguerre ensemble in deriving the HS and Bures volumes and hyperareas of  $n$ -level quantum systems [13, 14]. Generalized (associated/Sonine) Laguerre polynomials [“Laguerre functions”] have been employed in another important quantum-information context, in proofs of Page’s conjecture on the average entropy of a subsystem [43, 44].)

We, thus, have, for our two-qubit quaternionic case, that

$$R_2 = \frac{R_2^{numer}}{R_2^{denom}} = \frac{125769}{185725} \approx 0.677179. \quad (11)$$

(The *real* counterpart of  $R_2$  is  $\frac{1024}{135\pi^2} \approx 0.76854$ , and the *complex* one,  $\frac{71}{99} \approx 0.717172$ . Additionally, we computed that the corresponding “truncated” quaternionic [45] ratio—when *one* of the four quaternionic parameters is set to zero, that is the Dyson-index case  $\beta = 3$ —is  $\frac{726923214848}{106376244975\pi^2} \approx 0.692379$ . Thus, we see that these four important ratios  $R_2(\beta)$  monotonically decrease as  $\beta$  increases, and also, significantly, that the two ratios for odd values of  $\beta$  differ qualitatively—both having  $\pi^2$  in their denominators—from those two for even  $\beta$ .)

Our quasi-Monte Carlo (preliminary) estimate of the two-qubit quaternionic separability *probability* is, then,

$$P_{sep/quat}^{HS} \approx R_1 R_2 = 0.0813594. \quad (12)$$

Multiplying the total volume of the 27-dimensional convex set of two-qubit quaternionic states, given in the framework of Andai [16] by (2), by this result (12), we obtain the two-qubit quaternionic separable volume estimate  $V_{sep/quat}^{HS} \approx 2.38775 \cdot 10^{-19}$ .

Our 24-dimensional quasi-Monte Carlo integration procedure leads to a derived estimate of (the total 27-dimensional volume)  $V_{quat}^{HS}$ , that was somewhat smaller,  $2.85906 \cdot 10^{-18}$ , than the actual value  $2.93352 \cdot 10^{-18}$  given by (2). Although rather satisfying, this was sufficiently imprecise to discourage us from further attempting to “guestimate” the (all-important) constant ( $R_1$ ) by which to multiply the putative normalized form,  $(\frac{1}{2}(3 - \mu^2)\mu)^4$ , of the quaternionic separability function in (9) in order to yield the true separable volume. In our previous study [17, sec. IX.A], we presented certain plausibility arguments to the effect that the corresponding  $R_1$  constant in the 9-dimensional real case was  $\frac{135\pi^2}{2176} = (\frac{20\pi^4}{17})/(\frac{512\pi^2}{27})$ , and  $\frac{24}{71} = (\frac{256\pi^6}{639})/(\frac{32\pi^6}{27})$  in the 15-dimensional complex case. (This leads—multiplying by the corresponding  $R_2$ ’s,  $\frac{1024}{135\pi^2}$  and  $\frac{71}{99}$ —to separability probabilities of  $\frac{8}{17}$  and  $\frac{8}{33}$ , respectively.)

## 2. Supplementary estimation of $R_1$ constant

In light of such imprecision, in our initial estimates, we undertook a supplementary analysis, in which, instead of examining each feasible 24-dimensional TF point for 2,001 possible values of  $\mu$ , with respect to separability or not, we simply used  $\mu = 1$ . This, of course, allows us to significantly increase the number of points generated from the 64,000,000 so far employed.

We, thusly, generated 1,360,000,000 points, finding that we obtained a remarkably good fit to the important ratio  $R_1$  of the 24-dimensional measure ( $m_{sep}$ ), at  $\mu = 1$ , assigned to the separable two-qubit quaternionic density matrices to the (known) measure ( $m_{tot} = \frac{\pi^{12}}{7776000}$ ) by setting  $R_1 = (\frac{24}{71})^2 \approx 0.114263$  (our sample estimate of this quantity being the very close 0.114262). This is *exactly* the square of the corresponding ratio  $\frac{24}{71}$  we had conjectured (based on extensive numerical and theoretical evidence) for the full (15-dimensional) complex two-qubit case in [17].

### 3. Conjectured complex and quaternionic separability functions and probabilities

Under this hypothesis on  $R_1$  for  $\beta = 4$ , we have the ensuing string of relationships

$$\mathcal{S}_{quat}^{HS}(\mu) = \left(\frac{24}{71}\right)^2 \left(\frac{1}{2}(3 - \mu^2)\mu\right)^4 = \left(\frac{6}{71}\right)^2 \left((3 - \mu^2)\mu\right)^4 = \left(\mathcal{S}_{complex}^{HS}(\mu)\right)^2, \quad (13)$$

with (as already advanced in [17]),

$$\mathcal{S}_{complex}^{HS}(\mu) = \frac{24}{71} \left(\frac{1}{2}(3 - \mu^2)\mu\right)^2 = \frac{6}{71} \left((3 - \mu^2)\mu\right)^2. \quad (14)$$

Then, using our knowledge of the complementary ratio  $R_2$ , given in (11), we obtain the desired exact result,

$$P_{sep/quat}^{HS} = R_1 R_2 = \frac{72442944}{936239725} = \frac{2^6 \cdot 3^3 \cdot 7 \cdot 53 \cdot 113}{5^2 \cdot 17 \cdot 19 \cdot 23 \cdot 71^2} \approx 0.0773765, \quad (15)$$

(the complex counterpart being  $\frac{8}{33}$ ), as well as—in the framework of Andai [16]—that

$$V_{sep/quat}^{HS} = \frac{5989\pi^{12}}{24386773433626137413880000000} \approx 2.26986 \cdot 10^{-19}. \quad (16)$$

### B. Truncated quaternionic analysis ( $\beta = 3$ )

For possible further insight into the HS two-qubit separability probability question, we undertook a parallel quasi-Monte Carlo (Tezuka-Faure) integration (setting  $\mu = 1$ ) for the truncated quaternionic case ( $\beta = 3$ ), in which one of the four quaternionic parameters is set to zero. Although there was no corresponding formula for the HS total volume for this scenario given in [16], upon request, A. Andai kindly derived the result

$$V_{trunc}^{HS} = \frac{\pi^{10}}{384458588946432000} \approx 2.43584 \cdot 10^{-13}. \quad (17)$$

In fact, Andai was able to derive *one* simple overall comprehensive formula,

$$V_{n,\beta}^{HS} = \frac{\pi^{\frac{\beta n(n-1)}{4}}}{\Gamma(\beta \frac{n(n-1)}{2} + n)} \prod_{i=1}^{n-1} \Gamma\left(\frac{i\beta}{2} + 1\right) \quad (18)$$

yielding the total HS volumes for all  $n \times n$  systems and Dyson indices  $\beta$ . Let us, further, note that Andai obtains the result (17) as the product of three factors,  $V_{trunc}^{HS} = \pi_1 \pi_2 \pi_3$ , where

$$\pi_1 = \frac{128\pi^8}{105}; \quad \pi_2 = \frac{128}{893025}; \quad \pi_3 = \frac{189\pi^2}{12696335643836416}. \quad (19)$$

Now, we will simply *assume*—in line with our basic Dyson-index ansatz, substantially supported in [17] and above—that the corresponding separability function is of the form

$$\mathcal{S}_{trunc}^{HS}(\mu) \propto ((3 - \mu^2)\mu)^\beta, \quad \beta = 3. \quad (20)$$

(Of course, one should ideally *test* this specific application of the ansatz too, perhaps using the same quasi-Monte Carlo method we have applied to the  $\beta = 4$  instance above [Fig. 1].)

We were somewhat perplexed, however, by the results of our quasi-Monte Carlo integration procedure, conducted in the 18-dimensional space of off-diagonal entries of the truncated quaterionic density matrix  $\rho$ . Though, we anticipated (from our previous extensive numerical experience here and elsewhere) that the estimate of the associated 18-dimensional volume would be, at least, within a few percentage points of  $\pi_1\pi_2 = \frac{16384\pi^8}{93767625} \approx 1.65793$ , our actual estimate was, in fact, close to 0.967 (1, thus, falling within the possible margin of error). Assuming the correctness of the analysis of Andai, which we have no other reason to doubt, the only possible explanations seemed to be that we had committed some programming error (which we were unable to discern) or that we had some conceptual misunderstanding regarding the analysis of truncated quaternions. (Let us note that we do convert the  $4 \times 4$  density matrix to  $8 \times 8$  [complex] form [27, p. 495] [41, eq. (17)] [42, sec. II], while it appears that Andai does not directly employ such a transformation in his derivations.)

In any case, we did devote considerable computing time to the  $\beta = 3$  problem (generating 1,180,000,000 18-dimensional Tezuka-Faure points), with the hope being that if we were in some way in error, the error would be an *unbiased* one, and that the all-important *ratio* of separable to total volume would be unaffected.

Proceeding thusly, our best estimate (*not* making use of the Andai result (17) for the present) of the HS separability probability was 0.193006. One interesting possible candidate exact value is, then,  $\frac{128}{633} = \frac{2^7}{3 \cdot 13 \cdot 17} \approx 0.193062$ . (Note the presence of 128 in the numerators, also, of both factors  $\pi_1$  and  $\pi_2$ , given in (19).) This would give us a counterpart [ $\beta = 3$ ] value for the ratio  $R_2$  of  $\frac{160446825\pi^2}{5679087616} \approx 0.278838$ . In [17], we had asserted that, in the other odd  $\beta = 1$  case, the counterpart of  $R_2$  was  $\frac{135\pi^2}{2176} \approx 0.612315$ . (Multiplying this by  $\frac{1024}{135\pi^2}$  gave us the conjectured HS *real* two-qubit separability probability of  $\frac{8}{17}$ .)

So, let us say that although we believe we have successfully resolved—though still not having formal proofs—the two-qubit Hilbert-Schmidt separability probability question for the  $\beta = 2$  and 4 (complex and quaterionic) cases, the odd ( $\beta = 1, 3$ ) cases, in particular

$\beta = 3$ , appear at this point to be more problematical.

### C. Real and complex Qubit-Qutrit Hilbert-Schmidt Analyses

For qubit-qutrit systems, we have previously reported [17, eq. (44)], following the lines of our (Bloore-parameterization-based) two-qubit analyses, that rather than the use of one ratio variable  $\mu$ , in implementing the Peres-Horodecki positive-partial-transpose test for separability, it is necessary to employ two (corresponding specifically here to the case where the partial transpose is implemented by transposing the four  $3 \times 3$  blocks of the  $6 \times 6$  density matrix  $\rho$  in place) variables, already presented in (4).

Once again, employing the Tezuka-Faure quasi-Monte Carlo methodology, we generated 133,545 30-dimensional and 1,950,000 20-dimensional *feasible* points, corresponding now to the off-diagonal Bloore parameters of  $6 \times 6$  complex and real density matrices, respectively. (Each analysis was run on a MacMini workstation for a number of weeks.) The much larger number of feasible Tezuka-Faure points generated in the real case was primarily due to our reparameterization in that case of the Bloore off-diagonal entries (essentially correlations) in terms of *partial* correlations [20, 21, 22] (cf. [46]). This allowed us to somewhat mitigate the computational “curse” of high dimensionality, in that *each* sampled point now corresponds to a density matrix and *none* (theoretically, at least) has to be discarded. (H. Joe has demonstrated that it is possible to also implement this approach in the complex case, but the programming challenges for us were substantially greater, so we have not yet pursued such a course.) Of the 2,250,000 20-dimensional points, 38,622 were discarded because certain numerical difficulties (mainly convergence problems), arose in transforming to the partial correlations. The 133,545 feasible 30-dimensional points were drawn from (a much larger) 430,000,000 ones.

For each feasible sampled point we tested whether the associated (real or complex)  $6 \times 6$  density matrix was separable or not (that is, whether or not it passed the Peres-Horodecki test) for all possible pairs of  $\nu_1$  and  $\nu_2$  ranging from 0 to 1 in increments of  $\frac{1}{100}$ —that is,  $101^2 = 10,201$  Peres-Horodecki positive-partial-transpose tests were performed for *each* feasible sampled Tezuka-Faure point. We present the two estimated bivariate separability functions in Fig. 3 and Fig. 4 (cf. [17, Figs. 3, 5]).

In Fig. 5 we present a test of our Dyson-index HS separability-function ansatz by sub-

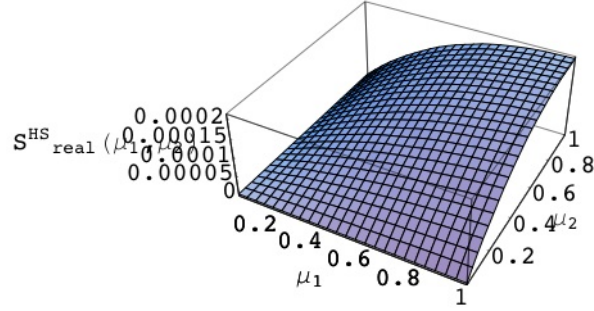


FIG. 3: Interpolated estimate over the unit square of the real qubit-qutrit separability function  $S_{real/qub-qut}^{HS}(\nu_1, \nu_2)$ , based on 2,211,378 20-dimensional Tezuka-Faure points. For *each* of these points, 10,201 associated  $6 \times 6$  density matrices, parameterized by  $\nu_1 \in [0, 1]$  and  $\nu_2 \in [0, 1]$ , were tested for separability.

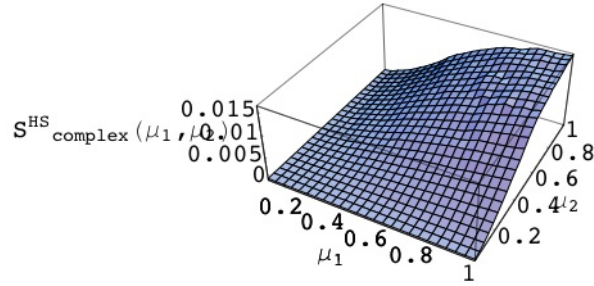


FIG. 4: Interpolated estimate over the unit square of the complex qubit-qutrit separability function  $S_{complex/qub-qut}^{HS}(\nu_1, \nu_2)$ , based on 133,545 *feasible* 30-dimensional Tezuka-Faure points. For each point, 10,201 associated  $6 \times 6$  density matrices, parameterized by  $\nu_1 \in [0, 1]$  and  $\nu_2 \in [0, 1]$ , were tested for separability.

tracting from Fig. 4 the *square* of the function in Fig. 3, which has been normalized so that its value at  $\nu_1 = 1, \nu_2 = 1$  equals that of the raw, unadjusted complex separability function. One should, of course, note the greatly-reduced  $z$ -axis scale from Fig. 4, indicating close

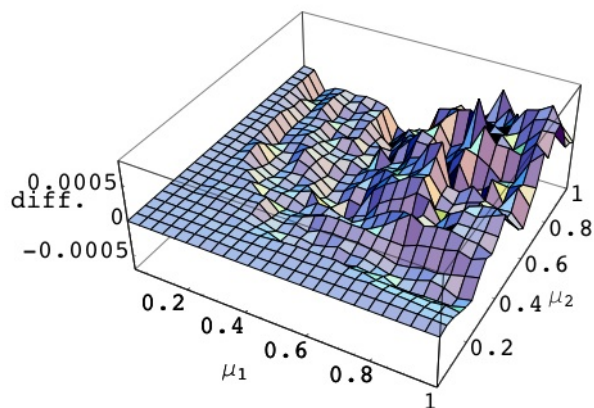


FIG. 5: The complex qubit-qutrit separability function shown in Fig. 4 minus the *square* of the real qubit-qutrit separability function (Fig. 4), the latter function normalized so that the value in the plot at  $\nu_1 = 1, \nu_2 = 1$  is 0. Note, importantly, the greatly-reduced  $z$ -axis scale *vis-à-vis* that of Fig. 4

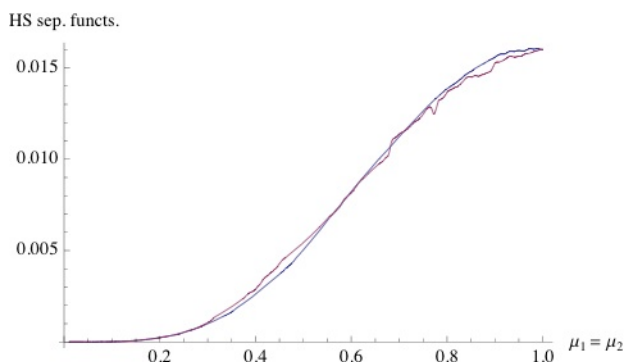


FIG. 6: The complex qubit-qutrit separability function (Fig. 4) and the normalized square of the real function (Fig. 3), holding  $\nu_1 = \nu_2$ . By construction, the two curves are equal at  $\nu_1 = \nu_2 = 1$ . The observed closeness of the two curves would be suggested by the HS Dyson-index ansatz

adherence to the HS Dyson-index separability-function ansatz, which it has been a principal goal of this study to test.

Now, in Fig. 6 we plot two very closely-fitting curves. One is the *complex* separability function holding  $\nu_1 = \nu_2$ , and the other, the *square* of the *real* separability function also holding  $\nu_1 = \nu_2$ , but normalized to equal the first (complex) function at the point  $(1, 1)$ . This is also compelling evidence for the validity of the HS Dyson-index ansatz.

Also, in [17], we indicated that it strongly appeared that though *two* ratio variables,  $\nu_1$

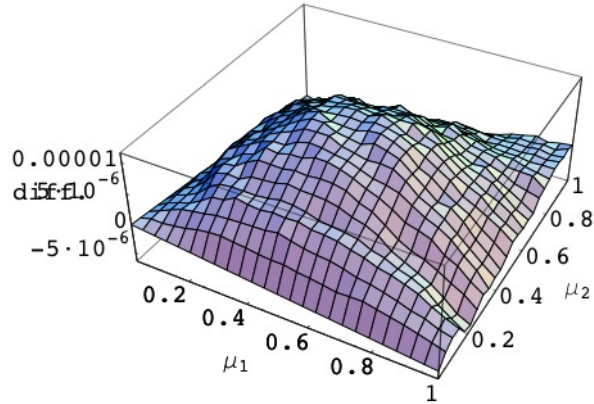


FIG. 7: The estimated qubit-qutrit real separability function (Fig. 3) minus the candidate function (22), the latter function being scaled so the plotted value at  $(\nu_1, \nu_2) = (1, 1)$  is 0.

and  $\nu_2$ , given in (4), are *ab initio* necessary in the qubit-qutrit analysis, it seems that upon further analysis they coalesce into a product

$$\eta = \nu_1 \nu_2 = \frac{\rho_{11} \rho_{66}}{\rho_{33} \rho_{44}}, \quad (21)$$

and the separability function problem becomes actually simply univariate in nature, rather than bivariate. This aspect needs, of course, to be more closely evaluated in light of our new numerical results. In fact, one candidate HS separability function of such a *univariate* nature which can be seen to fit our estimated functions (Figs. 3 and 4) both very well (when appropriately normalized and/or squared) is (Fig. 7)

$$\mathcal{S}_{real/qub-qut}^{HS}(\nu_1 \nu_2) \propto 1 - (1 - \nu_1 \nu_2)^{\frac{5}{2}} = 1 - (1 - \eta)^{\frac{5}{2}} = \frac{5}{2} B_{\eta}(1, \frac{5}{2}). \quad (22)$$

In Fig. 7 we show the fit of this function to the estimated qubit-qutrit real separability function (Fig. 3). In Fig. 8 we show the sum-of-squares of the fit of the one-parameter family of functions  $1 - (1 - \nu_1 \nu_2)^{\gamma}$  to the normalized estimated real qubit-qutrit separability function (Fig. 3). (For  $\gamma = \frac{5}{2}$  we obtain (22). We observe that the minimum of the curve is somewhat in the neighborhood of  $\gamma = \frac{5}{2}$ .)

In Fig. 9 we show the sum-of-squares of the fit of the *two*-parameter family of functions  $1 - (1 - (\nu_1 \nu_2)^{\theta})^{\gamma}$  to the normalized estimated real qubit-qutrit separability function (Fig. 3). (For  $\gamma = \frac{5}{2}, \theta = 1$  we obtain (22). We observe that the minimum of the curve is somewhat in the neighborhood of  $\gamma = \frac{5}{2}, \theta = 1$ .)

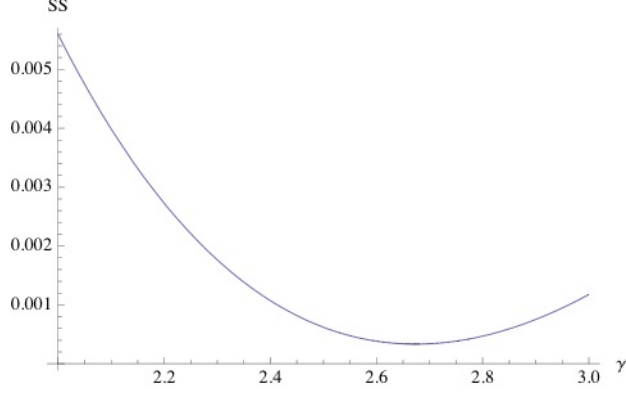


FIG. 8: The sum-of-squares (SS) of the fit of the one-parameter family of functions  $1 - (1 - \nu_1\nu_2)^\gamma$  to the normalized estimated real qubit-qutrit separability function (Fig. 3). For  $\gamma = 2.5$ , we obtain the candidate separability function (22)

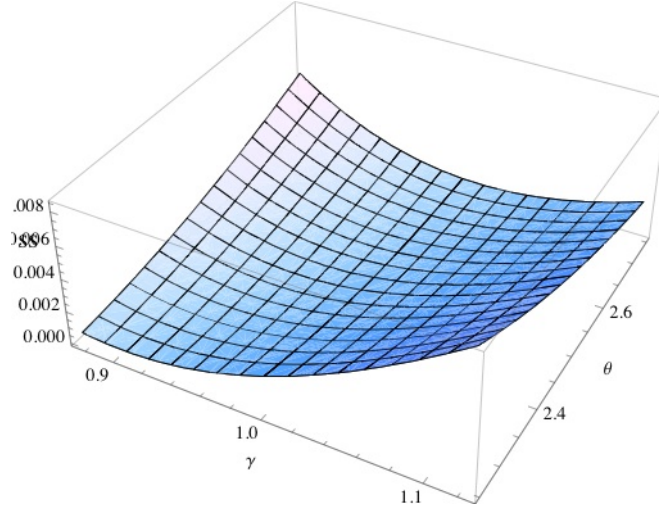


FIG. 9: The sum-of-squares (SS) of the fit of the *two*-parameter family of functions  $1 - (1 - (\nu_1\nu_2)^\theta)^\gamma$  to the normalized estimated real qubit-qutrit separability function (Fig. 3). For  $\gamma = 2.5, \theta = 1$ , we obtain the candidate separability function (22)

In the framework of Andai [16], the total volume of the 25-dimensional convex set of real  $6 \times 6$  density matrices can be represented as the product

$$V_{qub-qut/real}^{HS} = \frac{8192\pi^6}{253125} \cdot \frac{25\pi^3}{1399771004732964864} = \frac{\pi^9}{1730063650258944000} \approx 1.72301 \cdot 10^{-14} \quad (23)$$

and the total volume of the 35-dimensional convex set of complex  $6 \times 6$  density matrices as

the product

$$\begin{aligned}
V_{qub-qut/complex}^{HS} &= \frac{\pi^{15}}{86400000} \cdot \frac{1}{3460550346681745424512204800} \\
&= \frac{\pi^{15}}{298991549953302804677854494720000000} \approx 9.58494 \cdot 10^{-29}.
\end{aligned} \tag{24}$$

In both of these products, the first (20- or 30-dimensional) factor serves as the denominator of the ratio  $R_1$  and the second (5-dimensional) factor, as the denominator of the ratio  $R_2$ . (The numerator of  $R_1$  is the 20- or 30-dimensional mass assigned to the *separable* density matrices, and the numerator of  $R_2$  is the integral of the product of the corresponding suitably normalized separability function and Bloore jacobian over the 5-dimensional unit simplex.)

Under the assumption of the correctness of (22), we find that the qubit-qutrit counterparts of the important constants  $R_2$  employed above in the two-qubit case ((11) and immediately below there) are

$$R_{2_{qub-qut}}(\beta = 1) = 1 - \frac{4194304}{4849845\pi} \approx 0.724715, \tag{25}$$

$$R_{2_{qub-qut}}(\beta = 2) = \frac{-44632342463 + 68578836480 \log(2)}{4190140110} \approx 0.692789, \tag{26}$$

$$\begin{aligned}
R_{2_{qub-qut}}(\beta = 4) &= \\
&\frac{192210846322598002116984324520591 - 277301145703236210250598232096768 \log(2)}{501570554133080277487570824} \\
&\approx 0.675902,
\end{aligned} \tag{27}$$

for the real, complex and quaternionic cases, respectively. Again, we note a monotonic decrease as the Dyson index  $\beta$  increases. Also, for the truncated quaternionic ( $\beta = 3$ ) case, we found

$$\begin{aligned}
R_{2_{qub-qut}}(\beta = 3) &= \\
&\frac{967504709}{552123} - \frac{18446744073709551616(-67294453713397888 + 5638997741091\pi)}{71729672378917671400466262753675\pi^2} \\
&\approx 0.681261.
\end{aligned} \tag{28}$$

Our sample estimates of the complementary  $R_1$  constants were 0.226468, in the real case, and 0.047679 in the complex case. (We note that these estimates should be *independent* of the choice (correctness) of separability functions (22) and, in the complex case, the square of (22).) Forming the products  $R_1 R_2$  based on these estimates, we obtain an estimated real separability probability of 0.164125 and complex separability probability of 0.0330446.

Our numerical analyses have been concerned only with pairs of values of  $\nu_1$  and  $\nu_2$  lying within the (bounded) unit square  $[0, 1] \times [0, 1]$ . We have made the implicit assumption that the substance of our analyses would not be altered/biased if we were able to incorporate all possible pairs lying within the *unbounded* quadrant  $[0, \infty] \times [0, \infty]$ . (Clearly, for points  $\nu_1 > 1, \nu_2 > 1$ , simply by symmetry considerations, we immediately expect the separability function to be proportional to  $1 - (1 - \frac{1}{\eta})^{\frac{5}{2}}$ . For pairs of points  $(\nu_1, \nu_2)$  for which one member is greater than 1 and the other less than one, we expect the form the separability function takes to depend on whether or not  $\eta = \nu_1\nu_2 > 1$ .)

### 1. Relations to previous qubit-qutrit analyses [11, 17]

In [9], we had undertaken a large-scale numerical (again, Tezuka-Faure quasi-Monte Carlo integration) analysis of the separable volumes of the 35-dimensional convex set of *complex* qubit-qutrit systems, endowed with the Hilbert-Schmidt, as well as a number of monotone (including the Bures) metrics. The estimate we obtained there of the HS separability probability was 0.0266891. As we pointed out in our subsequent study [17, p. 14305], this is remarkably close to  $\frac{32}{1199} \approx 0.0266889$ .

In the subsequent study [17], which was chiefly devoted to the case of two-qubit systems, we had included supplementary analyses of the real and complex qubit-qutrit systems. But there we had only employed—in the interest of alacrity—Monte Carlo (random number), rather than (“lower-discrepancy”) quasi-Monte Carlo methods. So, the results presented in this paper, we believe should be more accurate and informative. (Also, rather than sampling grids for  $\nu_1, \nu_2$  of size  $101 \times 101$ , we had employed grids of sizes  $50 \times 50$  in the real case, and  $20 \times 20$  in the complex case.) In [17, sec. 10], we had put forth the tentative hypothesis that the corresponding real qubit-qutrit separability function was simply proportional to  $\sqrt{\eta} = \sqrt{\nu_1\nu_2}$  (having a somewhat similar profile to our present candidate (22), but definitely providing an inferior fit to our numerical results here).

## D. Bures two-qubit separability functions and probabilities

Now, in our present study, we shall somewhat parallel the sequential approach of Życzkowski and Sommers in that they, first, computed the *total* volume of (separable *and*

nonseparable)  $n \times n$  density matrices in terms of the (flat or Euclidean) Hilbert-Schmidt metric [13] [47, secs. 9.6-9.6, 14.3], and then, using the fundamentally important Bures (minimal monotone) metric [47, sec. 14.4] [14]. (In particular, they employed the Laguerre ensemble of random matrix theory [15] in both sets of computations (cf. [16]). The Bures and HS metrics were compared by Hall [48], who concluded that the Bures induced the “minimal-knowledge ensemble” (cf. [49]), also noting that in the single-qubit case, the Bures metric “may be recognized as the spatial part of the Robertson-Walker metric in general relativity”.) That is, we will seek now to extend the form of analysis applied in the Hilbert-Schmidt context in [17] to the Bures setting.

### 1. Review of earlier parallel Hilbert-Schmidt findings

To begin, let us review the most elementary findings reported in [17, sec. II.A.1]. The simplest (four-parameter) scenario studied there posits a  $4 \times 4$  density matrix  $\rho$  with fully general diagonal entries ( $\rho_{11}, \rho_{22}, \rho_{33}, \rho_{44} = 1 - \rho_{11} - \rho_{22} - \rho_{33}$ ) and only one pair of real off-diagonal non-zero entries,  $\rho_{23} = \rho_{32}$ . The HS separability function for that scenario was found to take the form [17, eq. (20)],

$$\mathcal{S}_{[(2,3)]}^{HS}(\mu) = \begin{cases} 2\mu & 0 \leq \mu \leq 1 \\ 2 & \mu > 1 \end{cases}, \quad (29)$$

where we primarily employ the variable  $\mu = \sqrt{\frac{\rho_{11}\rho_{44}}{\rho_{22}\rho_{33}}}$ , rather than  $\nu = \mu^2$ , as in [11, 17].

Allowing the 23- and 32-entries to be complex conjugates of one another, we further found for the corresponding separability function [17, eq. (22)]—where the wide tilde over an  $i, j$  pair will throughout indicate a complex entry (described by *two* parameters)—

$$\widehat{\mathcal{S}}_{[(2,3)]}^{HS}(\mu) = \left(\sqrt{\frac{\pi}{2}} \mathcal{S}_{[(2,3)]}^{HS}(\mu)\right)^2 = \begin{cases} \pi\mu^2 & 0 \leq \mu \leq 1 \\ \pi & \mu > 1 \end{cases}. \quad (30)$$

Further, permitting the 23- and 32-entries to be *quaternionic* conjugates of one another [27, 50], the corresponding separability function [17, eq. (24)]—where the wide hat over an  $i, j$  pair will throughout indicate a quaternionic entry (described by *four* parameters)—took

the form

$$\mathcal{S}_{[(2,3)]}^{HS}(\mu) = \left(\sqrt{\frac{\pi}{2}}\mathcal{S}_{[(2,3)]}^{HS}(\mu)\right)^2 = \left(\sqrt{\frac{\pi}{2}}\mathcal{S}_{[(2,3)]}^{HS}(\mu)\right)^4 = \begin{cases} \frac{\pi^2\mu^4}{2} & 0 \leq \mu \leq 1 \\ \frac{\pi^2}{2} & \mu > 1 \end{cases}. \quad (31)$$

So, the real (29), complex (30), and quaternionic (31) HS separability functions accord *perfectly* with the Dyson index sequence  $\beta = 1, 2, 4$  of random matrix theory [33]. “The value of  $\beta$  is given by the number of independent degrees of freedom per matrix element and is determined by the antiunitary symmetries . . . It is a concept that originated in Random Matrix Theory and is important for the Cartan classification of symmetric spaces” [51, p. 480]. The Dyson index corresponds to the “multiplicity of ordinary roots”, in the terminology of symmetric spaces [52, Table 2]. However, we remain unaware of any specific line of argument using random matrix theory [15] that can be used to formally confirm the HS separability function Dyson-index-sequence phenomena we have noted above and observed in [17]. (The basic difficulty/novelty appears to be that the separability aspect of the problem introduces a totally new set of complicated constraints—*quartic* (biquadratic) in  $\mu$  [17, eq. (5)] [11, eq. (7)]—that the multivariate integration must respect [17, sec. I.C].)

As a new exercise here, unreported in [17], we found that setting any single one of the four components of the quaternionic entry,  $x_{23} + \mathbf{i}y_{23} + \mathbf{j}ju_{23} + \mathbf{k}v_{23}$ , in the scenario just described, to zero, yields the (truncated quaternionic) separability function,

$$\mathcal{S}_{[(2,3)]}^{HS} = \begin{cases} \frac{4\pi\mu^3}{3} & 0 \leq \mu \leq 1 \\ \frac{4\pi}{3} & \mu > 1 \end{cases}, \quad (32)$$

consistent, at least, in terms of the exponent of  $\mu$ , with the Dyson-index pattern previously observed.

Continuing the analysis in [17], we computed the integrals

$$V_{sep/scenario}^{HS} = \int_0^\infty \mathcal{S}_{scenario}^{HS}(\mu)\mathcal{J}_{scenario}^{HS}(\mu)d\mu, \quad (33)$$

of the products of these separability functions with the corresponding (univariate) marginal jacobian functions (which are obtained by integration over diagonal parameters only and *not* any of the off-diagonal  $x_{ij}$ ’s and  $y_{ij}$ ’s) for the reparameterization of  $\rho$  using the Bloore variables [17, eq. (17)]. This yielded the HS scenario-specific *separable* volumes  $V_{sep/scenario}^{HS}$ .

The ratios of such separable volumes to the HS total volumes

$$V_{tot/scenario}^{HS} = c_{scenario}^{HS} \int_0^\infty \mathcal{J}_{scenario}^{HS}(\mu)d\mu, \quad (34)$$

where  $c_{scenario}^{HS}$  is a scenario-specific constant, gave us in [17] (invariably, it seems, exact) separability *probabilities*. (For the three scenarios listed above, these probabilities were, respectively,  $\frac{3\pi}{16}$ ,  $\frac{1}{3}$  and  $\frac{1}{10}$ .)

Based on the numerous scenario-specific analyses in [17], we are led to believe that the real, complex and quaternionic separability functions conform to the Dyson-index pattern for general scenarios, when the Hilbert-Schmidt measure has been employed. This apparent adherence was of central importance in arriving at the assertions in [17, secs. IX.A.1 and IX.A.2] that the HS separability probabilities of generic (9-dimensional] real) and (15-dimensional) complex two-qubit states are  $\frac{8}{17}$  and  $\frac{8}{33}$ , respectively. There we had posited—using mutually supporting numerical and theoretical arguments—that [17, eq. (102)]

$$\mathcal{S}_{real}^{HS}(\mu) \propto \frac{1}{2}(3 - \mu^2)\mu, \quad (35)$$

and, further pursuing our basic Dyson-index ansatz (fitting our numerical simulation extremely well [17, Fig. 4]), that  $(\mathcal{S}_{real}^{HS}(\mu))^2 \propto \mathcal{S}_{complex}^{HS}(\mu)$ . (Also, in the first part of the analyses above, we presented numerical evidence that  $(\mathcal{S}_{real}^{HS}(\mu))^4 \propto \mathcal{S}_{quat}^{HS}(\mu)$ , and made this relation more precise (13).)

## 2. Four-parameter density-matrix scenarios

Now, employing formulas (13) and (14) of Dittmann [53] for the *Bures* metric—which avoid the possibly problematical need for diagonalization of  $\rho$ —we were able to find the Bures volume elements for the same three basic (one pair of free off-diagonal entries) scenarios. We obtained for the real case,

$$dV_{[(2,3)]}^{Bures} = \frac{\sqrt{\rho_{11}}\sqrt{1 - \rho_{11} - \rho_{22}}\sqrt{\rho_{22}}}{4\sqrt{1 - x_{23}^2}(\rho_{22}\mu^2 + \rho_{11})\sqrt{\mu^2\rho_{22}^2 + (1 - \rho_{11})\rho_{11}}}d\rho_{11}d\rho_{22}dx_{23}d\mu, \quad (36)$$

for the complex case,

$$dV_{[(2,3)]}^{Bures} = \frac{\rho_{11}\rho_{22}(\rho_{11} + \rho_{22} - 1)}{4\sqrt{1 - y_{23}^2 - x_{23}^2}(\rho_{22}\mu^2 + \rho_{11})(-\rho_{11}^2 + \rho_{11} + \mu^2\rho_{22}^2)}d\rho_{11}d\rho_{22}dx_{23}dy_{23}d\mu, \quad (37)$$

and for the quaternionic case,

$$dV_{[(2,3)]}^{Bures} = \frac{A}{B}d\rho_{11}d\rho_{22}dx_{23}dy_{23}du_{23}dv_{23}d\mu, \quad (38)$$

where

$$A = -\rho_{11}^2\rho_{22}^2(\rho_{11} + \rho_{22} - 1)^2,$$

and

$$B = 4\sqrt{1 - u_{23}^2 - v_{23}^2 - x_{23}^2 - y_{23}^2} (\rho_{22}\mu^2 + \rho_{11}) (-\rho_{11}^2 + \rho_{11} + \mu^2\rho_{22}^2)^2.$$

In analyzing the quaternionic case, we transformed—using standard procedures [27, p. 495] [41, eq. (17)]—the corresponding  $4 \times 4$  density matrix into an  $8 \times 8$  density matrix with (only) complex entries. To this, we found it most convenient to apply—since its eigenvalues and eigenvectors could be explicitly computed—the basic formula of Hübner [54] [55, p. 2664] for the Bures metric.

Integrating these three volume elements over all the (four, five or seven) variables, while enforcing the nonnegative definiteness requirement for  $\rho$ , we derived the Bures *total* (separable *and* nonseparable) volumes for the three scenarios— $V_{tot/[(2,3)]}^{Bures} = \frac{\pi^2}{12} \approx 0.822467$ ,  $V_{tot/[(2,3)]}^{Bures} = \frac{\pi^3}{64} \approx 0.484473$ , and  $V_{tot/[(2,3)]}^{Bures} = \frac{\pi^4}{768} \approx 0.126835$ .

We note importantly that the Bures volume elements ((36), (37), (38)), in these three cases, can be *factored* into products of functions of the *off-diagonal* Bloore variables,  $u_{23}, v_{23}, x_{23}$  and  $y_{23}$ , and functions of the *diagonal* variables,  $\rho_{11}, \rho_{22}$  and  $\mu$ . Now, we will integrate (one may transform to polar and spherical coordinates, as appropriate) just the factors— $\frac{1}{\sqrt{1-x_{23}^2}}$ ,  $\frac{1}{\sqrt{1-x_{23}^2-y_{23}^2}}$  and  $\frac{1}{\sqrt{1-u_{23}^2-v_{23}^2-x_{23}^2-y_{23}^2}}$ —involving the off-diagonal variable(s) over those variables. In doing this, we will further enforce (using the recently-incorporated integration-over-implicitly-defined-regions feature of Mathematica) the Peres-Horodecki positive-partial-transpose-criterion [29, 30, 56], expressible as

$$\mu^2 - x_{23}^2 \geq 0 \tag{39}$$

in the real case,

$$\mu^2 - x_{23}^2 - y_{23}^2 \geq 0, \tag{40}$$

in the complex case, and

$$\mu^2 - x_{23}^2 - y_{23}^2 - u_{23}^2 - v_{23}^2 \geq 0, \tag{41}$$

in the quaternionic case. (None of the individual diagonal  $\rho_{ii}$ 's appears explicitly in these constraints, due to an attractive property of the Bloore [correlation coefficient/off-diagonal scaling] parameterization. Replacing  $\mu^2$  in these three constraints by simply unity, we obtain the non-negative definiteness constraints on  $\rho$  itself, which we also obviously must enforce.)

Performing the indicated three integrations, we obtain the *Bures* separability functions,

$$\mathcal{S}_{[(2,3)]}^{Bures}(\mu) = \begin{cases} \pi & \mu \geq 1 \\ 2 \sin^{-1}(\mu) & 0 < \mu < 1 \end{cases}, \quad (42)$$

$$\mathcal{S}_{[(2,3)]}^{Bures}(\mu) = \begin{cases} 2\pi & \mu \geq 1 \\ 2\pi \left(1 - \sqrt{1 - \mu^2}\right) & 0 < \mu < 1 \end{cases}, \quad (43)$$

and

$$\mathcal{S}_{[(2,3)]}^{Bures}(\mu) = \begin{cases} \frac{4\pi^2}{3} & \mu > 1 \\ \frac{2}{3}\pi^2 \left(-\sqrt{1 - \mu^2}\mu^2 - 2\sqrt{1 - \mu^2} + 2\right) & 0 < \mu < 1 \end{cases}. \quad (44)$$

Then, utilizing these three separability functions—that is, integrating the products of the functions and the corresponding remaining *diagonal*-variable factors in the Bures volume elements ((36), (37)), ((38)) over the  $\mu, \rho_{11}$  and  $\rho_{22}$  variables—we obtain *separable* volumes of  $V_{sep/[(2,3)]}^{Bures} = 0.3658435525$  and

$$V_{sep/[(2,3)]}^{Bures} = V_{tot/[(2,3)]}^{Bures} - \frac{1}{32}\pi^2(-2C + \pi) = \frac{1}{64}\pi^2(4C - 6 + \pi) \approx 0.124211 \quad (45)$$

and consequent separability *probabilities*, respectively, of 0.4448124200 and (our only *exact* Bures separability probability result in this study (cf. [6])),

$$P_{sep/[(2,3)]}^{Bures} = \frac{4C - 6 + \pi}{\pi} \approx 0.256384, \quad (46)$$

where  $C \approx 0.915966$  is Catalan's constant (cf. [57]). (This constant appears commonly in estimates of combinatorial functions and in certain classes of sums and definite integrals [58, sec. 1.7]. The ratio  $\frac{C}{\pi}$ —as well as having an interesting series expansion [58, p. 54]—occurs in exact solutions to the dimer problem of statistical mechanics [58, p. 54] [59, 60]).

Further, for the quaternionic case,  $V_{sep/[(2,3)]}^{Bures} \approx 0.012954754466$ , and  $P_{sep/[(2,3)]}^{Bures} \approx 0.10213883862$ . (The corresponding HS separability probability was also of the same relatively small magnitude, that is,  $\frac{1}{10}$  [17, sec. II.A.3]. We have computed the various Bures separable volumes and probabilities to high numerical accuracy, hoping that such accuracy may be useful in searches for possible further exact formulas for them.)

So, the normalized—to equal 1 at  $\mu = 1$ —forms of these three separability functions are  $\frac{\mathcal{S}_{[(2,3)]}^{Bures}(\mu)}{\pi}$ ,  $\frac{\mathcal{S}_{[(2,3)]}^{Bures}(\mu)}{2\pi}$  and  $\frac{3\mathcal{S}_{[(2,3)]}^{Bures}(\mu)}{4\pi^2}$ . In Fig. 10, we plot—motivated by the appearance of the Dyson indices in the analyses of [17]—the *fourth* power of the first (real) of these three

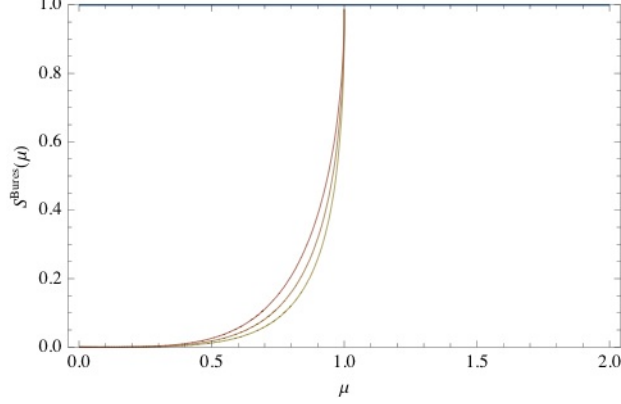


FIG. 10: Joint plot of the normalized Bures *quaternionic* separability function  $\frac{3\mathcal{S}_{[(2,3)]}^{Bures}(\mu)}{4\pi^2}$ , the *square* of the normalized Bures *complex* separability function  $\frac{\mathcal{S}_{[(2,3)]}^{Bures}(\mu)}{2\pi}$ , and the *fourth* power of the normalized Bures *real* separability function  $\frac{\mathcal{S}_{[(2,3)]}^{Bures}(\mu)}{\pi}$ . The order of dominance of the three curves is the same as the order in which they have been mentioned.

normalized functions together with the *square* of the second (complex) function and the (untransformed) third (quaternionic) function itself. We find a very close,

$$\left(\frac{\mathcal{S}_{[(2,3)]}^{Bures}(\mu)}{\pi}\right)^4 \approx \left(\frac{\mathcal{S}_{[(2,3)]}^{Bures}(\mu)}{2\pi}\right)^2 \approx \left(\frac{3\mathcal{S}_{[(2,3)]}^{Bures}(\mu)}{4\pi^2}\right), \quad (47)$$

but now *not* exact fit, as we did find in [17] for their (also normalized) Hilbert-Schmidt counterparts  $\frac{\mathcal{S}_{[(2,3)]}^{HS}(\mu)}{2}$ ,  $\frac{\mathcal{S}_{[(2,3)]}^{HS}(\mu)}{\pi}$  and  $\frac{2\mathcal{S}_{[(2,3)]}^{HS}(\mu)}{\pi^2}$  ((29), (30), (31)).

As an additional exercise (cf. (32)), we have computed the Bures separability function in the (truncated quaternionic) case that a single one of the four components of the (2,3)-quaternionic entry is set to zero. Then, we have (falling into the same tight cluster in Fig. 10, when the  $\frac{4}{3}$ -power of its normalized form is plotted)

$$\mathcal{S}_{[(2,3)]}^{Bures} = \begin{cases} \frac{1}{8}\pi^2 (4 - \sqrt{2} \log(3 + 2\sqrt{2})) & \mu > 1 \\ \frac{1}{4}\pi \left( \mu\sqrt{1 - \mu^2} - \sin^{-1}(\mu) \right) (\sqrt{2} \log(3 + 2\sqrt{2} - 4)) & 0 < \mu < 1 \end{cases}. \quad (48)$$

We have been able, further, using the formulas of Dittmann [53], to compute the Bures volume elements for the corresponding (five-dimensional) real and (seven-dimensional) complex scenarios, in which *both* the  $\{2, 3\}$  and  $\{1, 2\}$  entries are allowed to freely vary. But these volume elements do not appear, now, to fully factorize into products of functions (as is the case for (36) and (37)) involving just  $\rho_{11}, \rho_{22}, \mu$  and just the off-diagonal variables  $x_{ij}$ 's

and  $y_{ij}$ 's. The requisite integrations are, then, more problematical and it seemed impossible to obtain an explicit univariate separability function of  $\mu$ .

For instance, in this regard, we have for the indicated five-dimensional real scenario that

$$dV_{[(1,2),(2,3)]}^{Bures} = \frac{1}{4} \sqrt{\frac{A}{BC(D+E)}} d\rho_{11} d\rho_{22} dx_{12} dx_{23} d\mu, \quad (49)$$

where

$$A = -\rho_{11}^2 \rho_{22}^2 (\rho_{11} + \rho_{22} - 1) ((\mu^2 - 1) \rho_{22} + 1), \quad (50)$$

$$B = (\rho_{22} \mu^2 + \rho_{11})^2, C = x_{12}^2 + x_{23}^2 - 1, \quad (51)$$

$$D = (\rho_{11} + \rho_{22}) \left( x_{12}^2 \rho_{22} (\rho_{22} \mu^2 + \rho_{11})^2 - ((\mu^2 - 1) \rho_{22} + 1) (-\rho_{11}^2 + \rho_{11} + \mu^2 \rho_{22}^2) \right) \quad (52)$$

and

$$E = -x_{23}^2 \rho_{22} (\rho_{11} + \rho_{22} - 1) (-\rho_{11}^2 + \rho_{11} + \mu^2 \rho_{22}^2). \quad (53)$$

So, no desired factorization is apparent.

### 3. Five-parameter density-matrix scenarios

However, the computational situation greatly improves if we let the (1,4) and (2,3)-entries be the two free ones. (These entries are the specific ones that are interchanged under the operation of partial transposition, so there is a greater evident symmetry in such a scenario.) Then, we found that the three Bures volume elements all do factorize into products of functions of off-diagonal entries and functions of diagonal entries. We have

$$dV_{[(1,4),(2,3)]}^{Bures} = \frac{1}{8} \sqrt{\frac{1}{(x_{14}^2 - 1)(x_{23}^2 - 1)(\rho_{22} + \rho_{33} - 1)(\rho_{22} + \rho_{33})}} d\rho_{11} d\rho_{22} d\rho_{33} dx_{14} dx_{23}, \quad (54)$$

where simply for succinctness, we now show the volume elements before replacing the  $\rho_{33}$  variable by  $\mu$ . (We note that the expression for  $dV_{[(1,4),(2,3)]}^{Bures}$  is independent of  $\rho_{11}$ .) For the corresponding complex scenario,

$$dV_{[\widetilde{(1,4)}, \widetilde{(2,3)}]}^{Bures} = \frac{1}{8} \sqrt{\frac{F}{G}} d\rho_{11} d\rho_{22} d\rho_{33} dr_{14} dr_{23} d\theta_{14} d\theta_{23}, \quad (55)$$

where

$$F = -r_{14}^2 r_{23}^2 \rho_{11} \rho_{22} \rho_{33} (\rho_{11} + \rho_{22} + \rho_{33} - 1), \quad (56)$$

and

$$G = (r_{14}^2 - 1) (r_{23}^2 - 1) (\rho_{22} + \rho_{33} - 1)^2 (\rho_{22} + \rho_{33})^2, \quad (57)$$

and we have now further shifted to polar coordinates,  $x_{ij} + \mathbf{i}y_{ij} = r_{ij}(\cos \theta_{ij} + \mathbf{i} \sin \theta_{ij})$ .

For the quaternionic scenario, we have (using two sets of hyperspherical coordinates  $(r_{14}, \theta_{14}^{(1)}, \theta_{14}^{(2)}, \theta_{14}^{(3)})$  and  $(r_{23}, \theta_{23}^{(1)}, \theta_{23}^{(2)}, \theta_{23}^{(3)})$ ),

$$dV_{\widehat{[(1,4),(2,3)]}}^{Bures} = \frac{1}{8} \sqrt{\frac{\tilde{F}}{\tilde{G}}} d\rho_{11} d\rho_{22} d\rho_{33} dr_{14} dr_{23} d\theta_{14}^{(1)} d\theta_{14}^{(2)} d\theta_{14}^{(3)} d\theta_{23}^{(1)} d\theta_{23}^{(2)} d\theta_{23}^{(3)}, \quad (58)$$

where

$$\tilde{F} = \sin^2 \left( \theta_{14}^{(1)} \right) \sin \left( \theta_{14}^{(2)} \right) \sin^2 \left( \theta_{23}^{(1)} \right) \sin \left( \theta_{23}^{(2)} \right) r_{14}^3 r_{23}^3 \rho_{11}^{3/2} \rho_{22}^{3/2} (-\rho_{11} - \rho_{22} - \rho_{33} + 1)^{3/2} \rho_{33}^{3/2} \quad (59)$$

and

$$\tilde{G} = \sqrt{1 - r_{14}^2} \sqrt{1 - r_{23}^2} (\rho_{22} + \rho_{33} - 1)^2 (\rho_{22} + \rho_{33})^2. \quad (60)$$

The total Bures volume for the first (real) of these three scenarios is  $V_{tot/[(1,4),(2,3)]}^{Bures} = \frac{\pi^3}{64} \approx 0.484473$ , for the second (complex) scenario,  $V_{tot/[\widehat{(1,4)}, \widehat{(2,3)}]}^{Bures} = \frac{\pi^4}{192} \approx 0.507339$ , and for the third (quaternionic),  $V_{tot/[\widehat{[(1,4),(2,3)]}}^{Bures} = \frac{\pi^6}{245760} \approx 0.0039119$ .

In the two corresponding Hilbert-Schmidt (real and complex) analyses we have previously reported, we had the results [17, eq. (28)],

$$\mathcal{S}_{\widehat{[(1,4),(2,3)]}}^{HS}(\mu) = \begin{cases} 4\mu & 0 \leq \mu \leq 1 \\ \frac{4}{\mu} & \mu > 1 \end{cases}. \quad (61)$$

and [17, eq. (34)]

$$\mathcal{S}_{[\widehat{(1,4)}, \widehat{(2,3)}]}^{HS}(\mu) = \begin{cases} \pi^2 \mu^2 & 0 \leq \mu \leq 1 \\ \frac{\pi^2}{\mu^2} & \mu > 1 \end{cases}, \quad (62)$$

thus, exhibiting the indicated exact (Dyson-index sequence) proportionality relation. We now found, for the two Bures analogs, that

$$\mathcal{S}_{\widehat{[(1,4),(2,3)]}}^{Bures}(\mu) = \begin{cases} \pi^2 & \mu = 1 \\ 2\pi \csc^{-1}(\mu) & \mu > 1 \\ 2\pi \sin^{-1}(\mu) & 0 < \mu < 1 \end{cases}, \quad (63)$$

$$\mathcal{S}_{[(1,4),\widetilde{(2,3)}]}^{Bures}(\mu) = \begin{cases} 16\pi^2 & \mu = 1 \\ 16\pi^2 \left(1 - \frac{\sqrt{\mu^2-1}}{\mu}\right) & \mu > 1 \\ 16\pi^2 \left(1 - \sqrt{1-\mu^2}\right) & 0 < \mu < 1 \end{cases}, \quad (64)$$

and, further still, for the quaternionic scenario,

$$\mathcal{S}_{[(1,4),\widetilde{(2,3)}]}^{Bures}(\mu) = \begin{cases} \frac{16\pi^4}{9} & \mu = 1 \\ -\frac{8\pi^4 \left(2(\sqrt{\mu^2-1}-\mu)\mu^2 + \sqrt{\mu^2-1}\right)}{9\mu^3} & \mu > 1 \\ \frac{8}{9}\pi^4 \left(-\sqrt{1-\mu^2}\mu^2 - 2\sqrt{1-\mu^2} + 2\right) & 0 < \mu < 1 \end{cases}. \quad (65)$$

Employing these several results, we obtained that  $V_{sep/[(1,4),\widetilde{(2,3)}]}^{Bures} \approx 0.1473885131$ ,  $V_{sep/[(1,4),\widetilde{(2,3)}]}^{Bures} \approx 0.096915844$ , and  $V_{sep/[(1,4),\widetilde{(2,3)}]}^{Bures} \approx 0.000471134100$  giving us real, complex and quaternionic separability probabilities of 0.3042243652, 0.19102778 and 0.120436049.

We see that for values of  $\mu \in [0, 1]$ , the *normalized* forms of these three Bures separability functions are *identical* to the three obtained above ((42), (43), (44)) for the corresponding *single-nonzero-entry* scenarios. While those earlier functions were all constant for  $\mu > 1$ , we now have symmetrical behavior about  $\mu = 1$  in the form,  $\mathcal{S}_{scenario}^{Bures}(\mu) = \mathcal{S}_{scenario}^{Bures}\left(\frac{1}{\mu}\right)$ .

In Fig. 11, we show the analogous plot to Fig. 10, using the normalized (to equal 1 at  $\mu = 1$ ) forms of the three additional Bures separability functions ((63), (64), (65)). We again, of course, observe a very close fit to the type of proportionality relations *exactly* observed in the Hilbert-Schmidt case ((61), (62)).

We were, further, able to compute the Bures volume element for the *three-nonzero-entries* complex scenario  $[(\widetilde{1,2}), (\widetilde{1,4}), (\widetilde{2,3})]$ , but it was considerably more complicated in form than those reported above, so no additional analytical progress seemed possible.

#### 4. Additional analyses

Regarding the possible computation of Bures separability functions for the *totality* of 9-dimensional real and 15-dimensional complex two-qubit states, we have found, preliminarily, that the corresponding metric tensors (using the Bloore parameterization [sec. IA]) decompose into  $3 \times 3$  and  $6 \times 6$ , and  $3 \times 3$  and  $12 \times 12$  blocks, respectively. The  $3 \times 3$  blocks themselves are identical in the two cases, and of precisely the (simple diagonal) form (if we employ hyperspherical coordinates) that Akhtarshenas found for the Bures metric using the

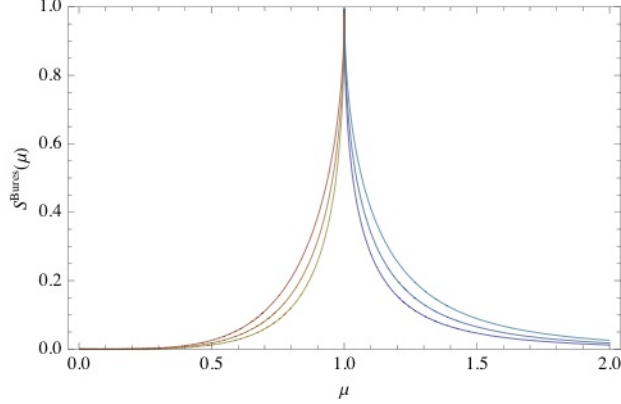


FIG. 11: Joint plot of the normalized Bures *quaternionic* separability function  $\frac{9S_{[(1,4),(2,3)]}^{Bures}(\mu)}{4}$ , the *square* of the normalized Bures *complex* separability function  $\frac{S_{[(1,4),(2,3)]}^{Bures}(\mu)}{16\pi^2}$ , and the *fourth* power of the normalized Bures *real* separability function  $\frac{S_{[(1,4),(2,3)]}^{Bures}(\mu)}{\pi^2}$ . Over the interval  $\mu \in [0, 1]$ , the three functions are identical—with the same order of dominance—to those in Fig. 10.

coset parameterization [61, eq. (23)]. These  $3 \times 3$  blocks, thus, depend only upon the diagonal entries (while in [61], the dependence, quite differently, was upon the eigenvalues). It appears, though, that the determinants—for which we presently lack succinct formulas—of the complementary  $6 \times 6$  and  $12 \times 12$  blocks, do depend upon all, diagonal and non-diagonal, parameters, rendering further analytical progress, along the lines pursued with substantial success for the Hilbert-Schmidt metric, for these scenarios rather problematical.

## 5. Discussion

The close proximity observed above between certain two-qubit separability results for the Hilbert-Schmidt and Bures metrics is perhaps somewhat similar in nature/explanation to a form of high similarity also observed in our previous analysis [9]. There, large scale numerical (quasi-Monte Carlo) analyses strongly suggested that the ratio of Hilbert-Schmidt separability probabilities of generic (rank-6) qubit-qutrit states ( $6 \times 6$  density matrices) to the separability probabilities of generically minimally degenerate (boundary/rank-5) qubit-qutrit states was equal to 2. (This has since been formally confirmed and generalized—in terms of positive-partial-transpose-ratios—to arbitrary bipartite systems by Szarek, Bengtsson and Życzkowski in [62]. They found that the set of positive-partial-transpose states is “pyramid decomposable” and, hence, is a body of constant height.) Parallel numerical ratio

estimates also obtained in [9] based on the Bures (and a number of other monotone) metrics were also surprisingly close to 2, as well (1.94334 in the Bures case [9, Table IX]). However, no exact value for the Bures qubit-qutrit ratio has yet been established, and our separability function results above, might be taken to suggest that the actual Bures ratio is not exactly equal to 2, but only quite close to it. (Possibly, in these regards, the Bures metric might profitably be considered as some perturbation of the flat Euclidean metric (cf. [63]).)

Further study of the forms the Bures separability functions take for qubit-qubit and qubit-qutrit scenarios is, of course, possible, with the hope that one can gain as much insight into the nature of Bures separability probabilities as has been obtained by examining the analogous Hilbert-Schmidt separability functions [17]. (In [8], we had formulated, based on extensive numerical evidence, conjectures—involving the silver mean,  $\sqrt{2} - 1$ —for the Bures [and other monotone metric] separability probabilities of the 15-dimensional convex set of [complex] qubit-qubit states, which we would further aspire to test. One may also consider the use of monotone metrics other than the *minimal* Bures one [16]—such as the Kubo-Mori and Wigner-Yanase.) The analytical challenges to further progress, however, in light of the apparent non-factorizability of volume elements into diagonal and off-diagonal terms, appear quite formidable.

### III. EULER-ANGLE-PARAMETERIZATION SEPARABILITY FUNCTIONS

In the previous section (sec. IID), we found that the Bloore parameterization (sec. IA), markedly useful in determining separable volumes based on the (non-monotone) Hilbert-Schmidt metric, is less immediately fruitful when the Bures (and presumably other monotone) metrics is employed. In light of this development, it appeared to be of interest to see if some other parameterizations might prove amenable to such type of “separability function” analyses. In particular, we will examine here the use for such purposes—as earlier suggested in [34]—of the  $SU(4)$  Euler-angle parameterization of the 15-dimensional complex set of  $4 \times 4$  density matrices developed by Tilma, Byrd and Sudarshan [31]. (We will closely follow the notation and terminology of [31]. In [34], we simply attempted to fit symmetric polynomials [64] to yield previously-conjectured separable volumes, and did not initiate any independent quasi-Monte Carlo estimation procedures, as we will immediately below.)

### A. Complex two-qubit case

The fifteen parameters, then, employed will be twelve Euler angles ( $\alpha_i$ 's) and three independent eigenvalues ( $\lambda_1, \lambda_2, \lambda_3$ ). The *total* (separable *and* nonseparable) volume is simply (for all metrics of interest) the *product* of integrals over these two sets of parameters [13, 14]. Now, to study the separable-volume question, in complete analogy to our methodology above, we would like to integrate over the twelve Euler angles (rather than the off-diagonal Bloore parameters, as before), while enforcing the positivity of the partial transpose, required for separability. We were, fortunately, able to perform such enforcement in the Bloore-parameterization case employing only a *single* diagonally-related parameter ( $\mu$ ), given in (3). Such a reduction in the number of relevant parameters, however, does not seem possible in the Euler-angle parameterization case. So, the analogue of the separability function we will obtain here will be a *trivariate* function (of the three eigenvalues). Hopefully, we will be able to determine an exact functional form for it, and then utilize it in further integrations to obtain separable volumes, in terms of both monotone and non-monotone metrics. (Also, the question of whether counterpart Euler-angle separability functions in the real and quaternionic cases adhere to some form of Dyson-index-sequence behavior certainly merits attention.)

### B. Trivariate separability function for volume computation

Now, we made use of a sequence of 1,900,000 12-dimensional Tezuka-Faure points (twelve being the number of Euler angles over which we will integrate). For each such point, we let the associated three (free) eigenvalues each take on all possible values from  $\frac{1}{40}$  to 1, in steps of  $\frac{1}{40}$ . Of course, the possible triads of free eigenvalues is constrained by the requirement that they not all sum to more than 1. There were 9,880 such possible triads. For each such triple—holding the Euler angles constant—we evaluated whether the associated  $4 \times 4$  density matrix was separable or not.

We, then, interpolated the results to obtain functions defined over the three-dimensional hypercube  $[0, 1]^3$ . In Fig. 12, we show a two-dimensional marginal section (over  $\lambda_1, \lambda_2$ , say) of this function (obtained by summing over the values of  $\lambda_3$ ) of the estimated three-dimensional separability function. We know from the work of Pittenger and Rubin [65, Cor.

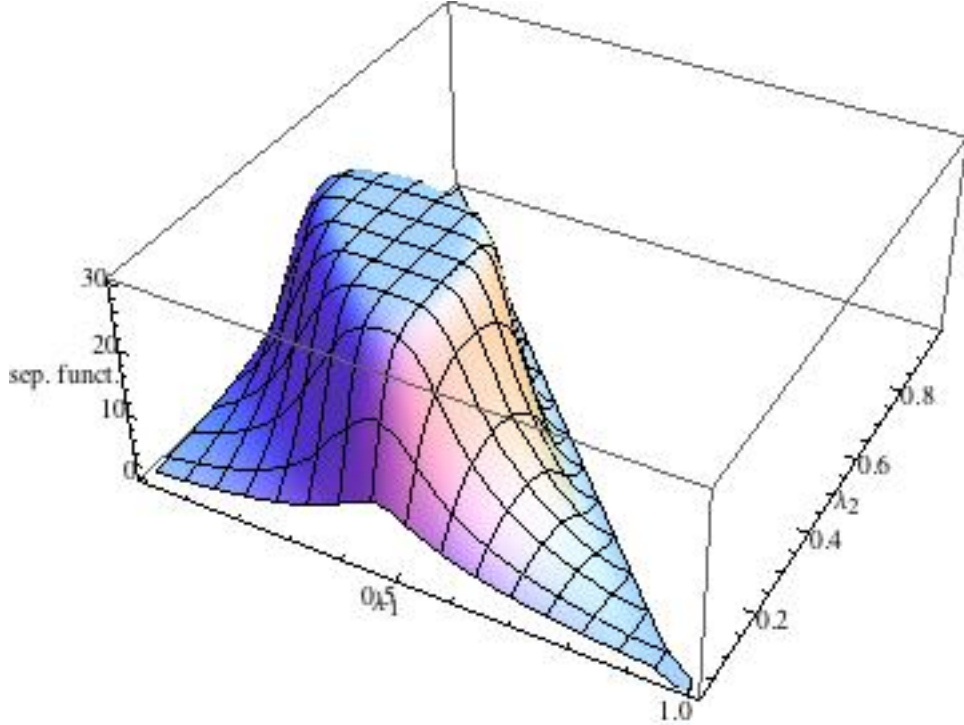


FIG. 12: Two-dimensional marginal section of the estimated three-dimensional separability function based on the Euler-angle parameterization for the 15-dimensional convex set of complex  $4 \times 4$  density matrices. Note the mesa/plateau shape, indicative of the fully separable neighborhood of the fully-mixed state

4.2], for example, that, for the specific case of two-qubits, any density matrix all of the four eigenvalues of which are greater than  $\frac{7}{30} \approx 0.2333$  *must* be separable. Therefore, there certainly does exist a neighborhood of the fully-mixed state (having its four eigenvalues equal to  $\frac{1}{4}$ ) that is composed of only separable states. This is reflected in the plateau present in Fig.. 12.

In Fig. 13 we, additionally display a one-dimensional marginal section (over  $\lambda_1$ ), obtained by summing over both  $\lambda_1$  and  $\lambda_2$ , of the estimated three-dimensional separability function. (The curve now appears unimodal rather than flat at its maximum,)

Employing the trivariate separability function obtained by interpolation from the data we have generated here, we were able to obtain an estimate of 0.242021 for the HS separability probability. (From our extensive Bloore-parameterization analyses, as previously noted we believe its true value is  $\frac{8}{33} \approx 0.242424$ .) We were essentially just as readily able to obtain an estimate of the Bures (minimal monotone) separability probability (or any of the

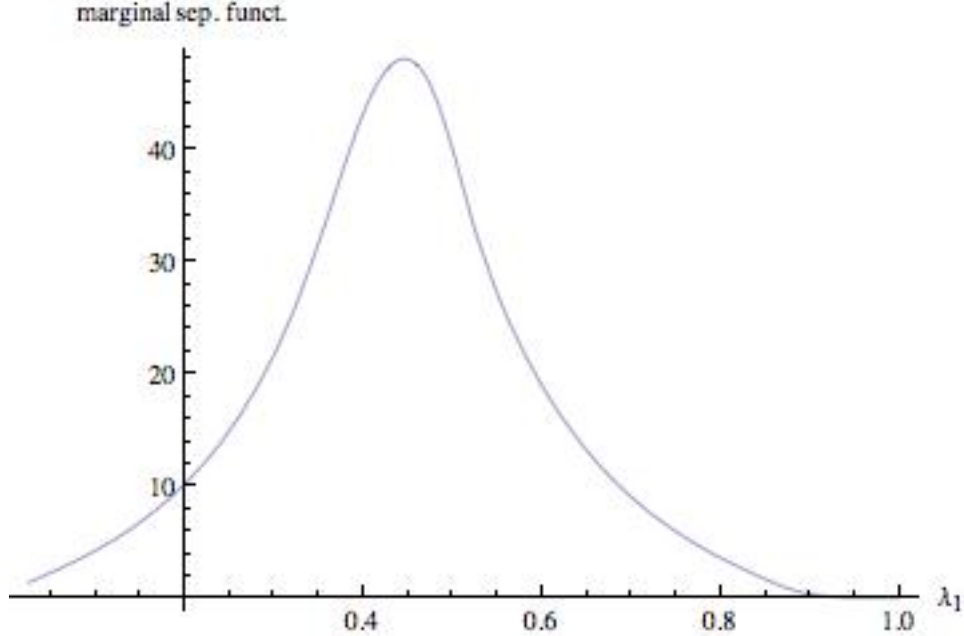


FIG. 13: One-dimensional marginal section of the estimated three-dimensional separability function based on the Euler-angle parameterization for the 15-dimensional convex set of complex  $4 \times 4$  density matrices

other monotone metrics—Kubo-Mori, Wigner-Yanase, . . . [66], it appears) of 0.0734223, while in [8], this had been conjectured to equal  $\frac{1680(-1+\sqrt{2})}{\pi^8} \approx 0.733389$ . (In the HS and Bures computations reported here and in the next section, we perform numerical integrations over the simplices of eigenvalues, in which the integrands are the products of our interpolated separability functions and the appropriate scenario-specific volume elements indicated in the twin Sommers-Życzkowski 2003 papers [13, 14].)

Of course, now the research agenda should turn to the issue of finding a possibly exact formula (undoubtedly *symmetric* in the three eigenvalues [34, secs. V and VI]) for this three-dimensional Euler-angle-based separability function, and for other qubit-qubit and qubit-qutrit scenarios.

In Fig. 14 we show, based on the 9,880 points sampled for each 12-dimensional TF-point, the estimated value of the separability function for that point *paired* with the Euclidean distance of the vector of eigenvalues  $(\lambda_1, \lambda_2, \lambda_3, 1 - \lambda_1 - \lambda_2 - \lambda_3)$  for that point from the vector of eigenvalues  $(\frac{1}{4}, \frac{1}{4}, \frac{1}{4}, \frac{1}{4})$ , corresponding to the fully mixed state.

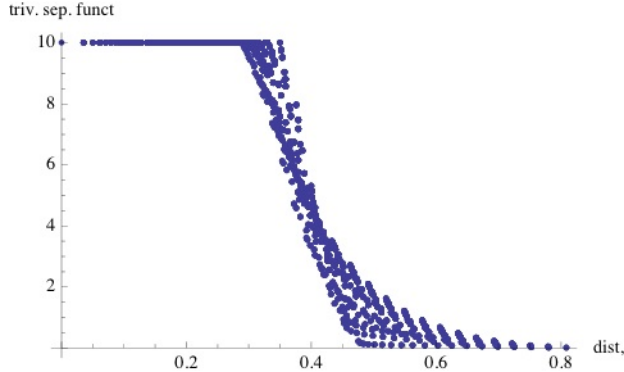


FIG. 14: The trivariate Euler-angle complex qubit-qubit separability function paired with the *Euclidean distance* of the corresponding vector of eigenvalues to the vector  $(\frac{1}{4}, \frac{1}{4}, \frac{1}{4}, \frac{1}{4})$ , corresponding to the fully mixed state

### C. *Bivariate separability function for area computation*

Now we repeat the procedures described immediately before, except for the *a priori* setting of *one* of the three free eigenvalues to zero, so the associated density matrices must lie on the 14-dimensional boundary of the 15-dimensional convex set of two-qubit complex states. (The analysis was conducted independently of that pertaining to the volume, and now we were able to employ a much larger number—23,500,000—of TF-points.) The resulting separability function is now bivariate, lending itself immediately to graphic display. In Fig. 15 we show this function, and in Fig. 16, its one-dimensional section over  $\lambda_1$ .

Employing the bivariate separability function (Fig. 15) obtained by interpolation from the data (23,500,000 TF-points) we generated, we were able to obtain an estimate of 0.12119 for the HS separability probability, which, from our complementary Bloore analyses, together with the (“one-half”) Theorem 2 of [62], we believe to be exactly  $\frac{4}{33} \approx 0.121212$ . (The proximity of our estimate to this value clearly serves to further fortify our conjecture that the HS separability probability of generic complex two-qubit states is  $\frac{8}{33}$ .) Additionally, our estimate of the associated *Bures* separability probability was 0.0396214, *approximately* one-half that of the corresponding probability for the non-degenerate complex two-qubit states [9].

In Fig. 17 we show, based on 780 points sampled for each 12-dimensional TF-point, the estimated value of the bivariate separability function for that point paired with the Euclidean distance of the vector of eigenvalues for that point from the vector of eigenvalues  $(\frac{1}{3}, \frac{1}{3}, \frac{1}{3}, 0)$

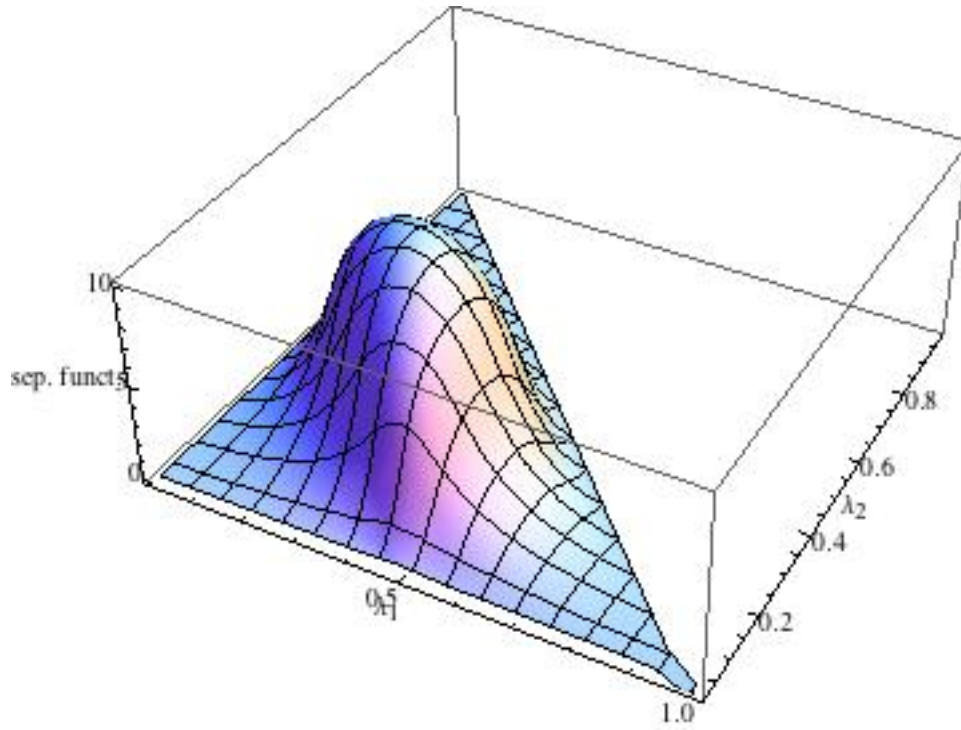


FIG. 15: Bivariate Euler-angle separability function for the 14-dimensional boundary hyperarea of the 15-dimensional convex set of complex  $4 \times 4$  density matrices

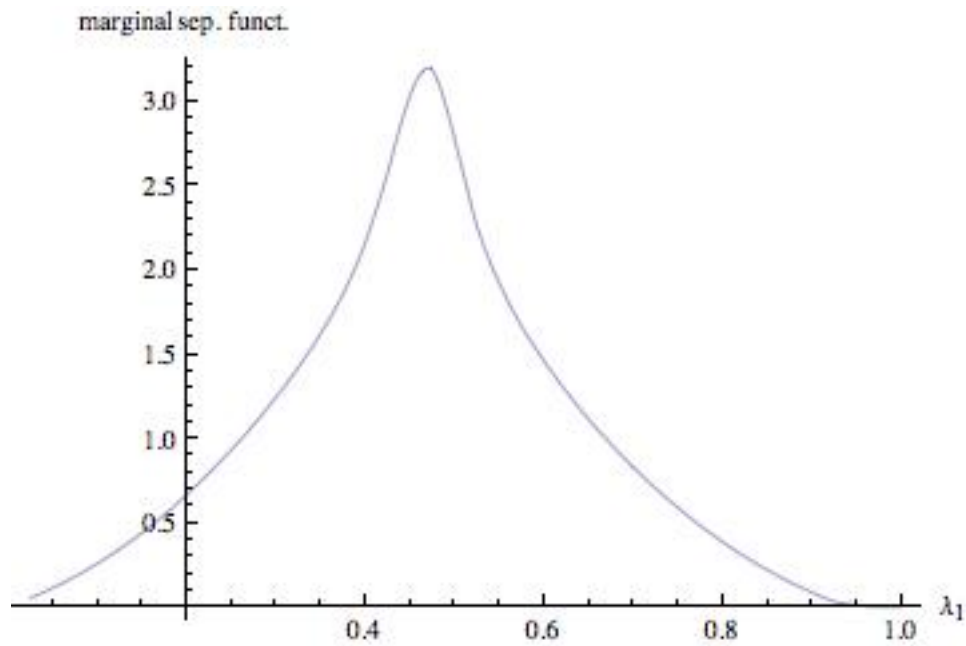


FIG. 16: One-dimensional marginal section of the estimated two-dimensional Euler-angle-based separability function for the 14-dimensional hyperarea of the 15-dimensional convex set of complex  $4 \times 4$  density matrices

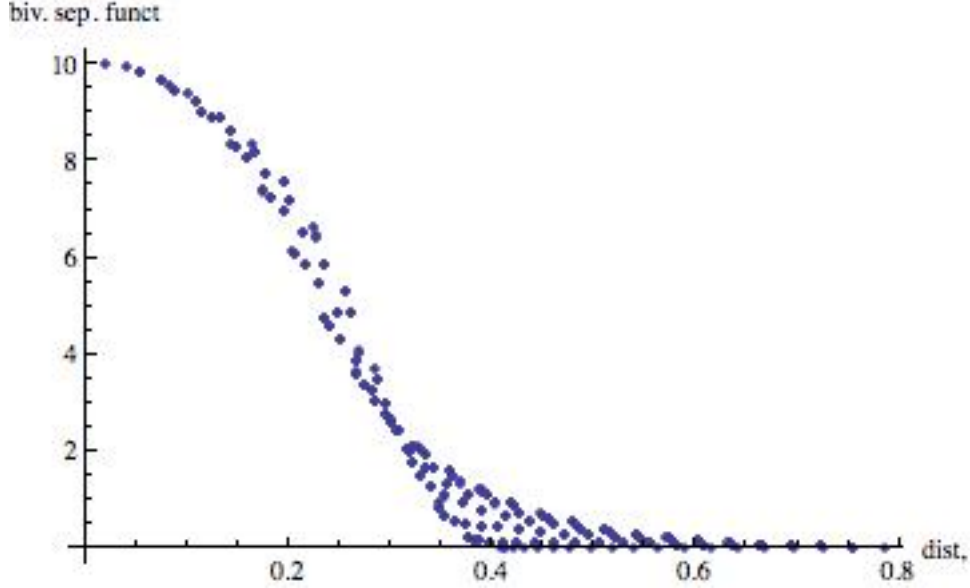


FIG. 17: Paired values of the estimated bivariate Euler-angle separability function (Fig. 15) and the *Euclidean distance* of the associated vector of eigenvalues to the vector  $(\frac{1}{3}, \frac{1}{3}, \frac{1}{3}, 0)$  corresponding to the most fully mixed boundary state

corresponding to the most fully mixed boundary state.

#### D. Participation ratios

The *participation ratio* of a state  $\rho$  is defined as [1, eq. (17)] [47, eq. (15.61)] [67, 68]

$$R(\rho) = \frac{1}{\text{tr}\rho^2}. \quad (66)$$

For  $R(\rho) > 3$ , a two-qubit state *must* be separable. For convenience, we will also employ the variable

$$S(\rho) = \frac{3}{2}\left(1 - \frac{1}{R(\rho)}\right), \quad (67)$$

which varies over the interval  $[0,1]$  for states *outside* the separable ball. In Fig. 18 we show a plot—having set *one* of the four eigenvalues to zero—of the sixth-power of this ratio. We note a close similarity in its shape to the estimated bivariate separability function displayed in Fig. 15. Although we can not similarly visually display the trivariate separability function we have found that it is closely fit—outside the separable ball ( $R(\rho) > 3$ ) [47, Fig. 15.7]—by the fourth-power of the participation ratio. In Fig. 19, we show the trivariate separability function *vs.*  $R(\rho)^4$ . (For  $R(\rho)^4 > 81$ , only separable states are encountered). In Fig. 20, we

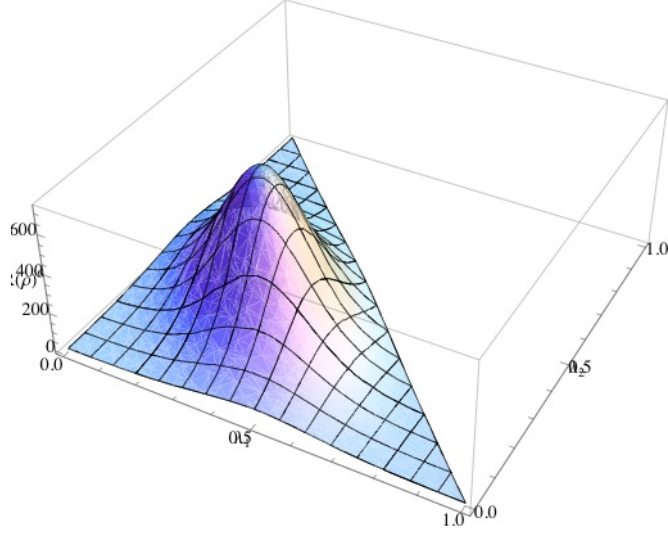


FIG. 18: The sixth-power,  $R(\rho)^6$ , of the participation ratio for minimally degenerate two-qubit states with one eigenvalue equal to zero. Note the similarity to Fig. 15

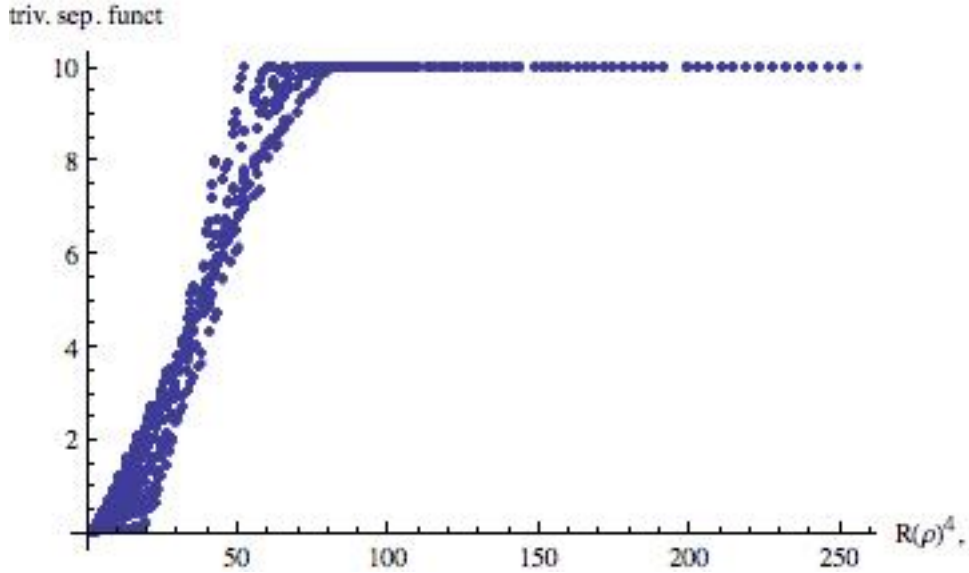


FIG. 19: The (Euler-angle) trivariate separability function for generic (15-dimensional) complex two-qubit states plotted against the fourth-power of the participation ratio for the 9,880 points sampled

show the comparable bivariate separability function *vs.*  $R(\rho)^6$ .

As an exercise (not directly tied to our quasi-Monte Carlo computations), we assumed that the trivariate Euler-angle separability functions are all proportional (outside the separable ball,  $R(\rho) > 3$ ) to some powers of  $R(\rho)$ , for each of the generic real, complex, truncated

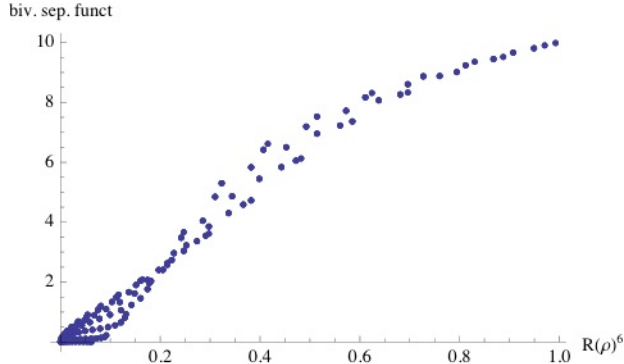


FIG. 20: The (Euler-angle) bivariate separability function for generic (14-dimensional) minimally degenerate complex two-qubit states plotted against the sixth-power of the participation ratio for the 780 points sampled

quaternionic and quaternionic two-qubit states. Then, we found those powers which fit our conjectured values (discussed in sec. II) for the associated Hilbert-Schmidt two-qubit separability probabilities. The powers we found were 1.36743 ( $\beta = 1$ ), 2.36904 ( $\beta = 2$ ) and 4.0632 ( $\beta = 4$ ). We observe here a rough approximation to Dyson-index behavior, but can speculate that when and if the true forms of the Euler-angle separability functions are found, such behavior will be strictly adhered to. (In fact, one research strategy might be to seek functions that fully conform to this principle, while fitting the conjectured HS separability probabilities. Also, below we will find closer adherence when we switch from the use of the participation ratio to a simple linear transform of the Verstraete-Audenaert-De Moor-function [69] (cf. [70]), which provides an improved bound on separability.)

When we similarly sought to fit our prediction of  $\frac{4}{33}$  (that is, one-half of  $\frac{8}{33}$  by the results of [62]) for the HS separability probability of generic minimally degenerate complex two-qubit states to a bivariate function proportional to a power of the participation ratio, we obtained a power of 6.11646, according rather well with Fig. 20.

In terms of the Hilbert-Schmidt metric, the lower bound on the complex two-qubit separability probability provided by the separable ball ( $R(\rho) > 3$ ) is rather small, that is  $\frac{35\pi}{23328\sqrt{3}} \approx 0.00272132$ , while relying upon the improved inequality reported in [69],

$$VAD(\rho) = \lambda_1 - \lambda_3 - 2\sqrt{\lambda_2\lambda_4} < 0, \quad (\lambda_1 > \lambda_2 > \lambda_3 > \lambda_4), \quad (68)$$

it is 0.00365406. These figures are both considerably smaller than the comparable ones (0.3023 and 0.3270) given in [69] using (apparently) the measure (*uniform* on the simplex

of eigenvalues) first employed in [1].

### E. Verstraete-Audenaert-De Moor function

If we switch from the participation ratio  $R(\rho)$  to a simple linear transformation of the Verstraete-Audenaert-De Moor function, that is,  $1 - VAD(\rho)$  (which varies over  $[0,1]$  for states outside the separable VAD set), in seeking to fit the trivariate separability function to our conjectured Hilbert-Schmidt two-qubit separability probabilities (sec. II), we find that in the generic complex ( $\beta = 2$ ) case,  $\left(1 - VAD(\rho)\right)^{3.15448}$  gives the best fit (for  $VAD(\rho) > 0$ ). Then, closely consistent with Dyson-index behavior, we obtained  $\left(1 - VAD(\rho)\right)^{1.53785}$  as the best fit in the generic real ( $\beta = 1$ ) scenario. (The VAD-bound (68) provides us with no useful information if we set  $\lambda_4 = 0$ , so no relevance to the minimally degenerate two-qubit scenario is apparent.)

### F. Beta function fits to Euler-angle separability functions

We can fit within 0.4% our conjectured values of  $\frac{4}{33}$  and  $\frac{4}{17}$  for the Hilbert-Schmidt separability probabilities of the complex and real minimally degenerate two-qubit states, respectively, by assuming—in line with the Dyson-index ansatz—that the Euler-angle separability function in the *real* case is a *regularized beta function* (incomplete beta function ratio) [32, p. 11] of the form  $I_{S(\rho)^2}(58, 22)$  (Fig. 21), *and* the Euler-angle separability function (Fig. 15) in the *complex* case, the *square* of that function. (Continuing along such lines, if we employ the fourth-power of the function, our estimate of the associated quaternionic separability probability is some 91.45% of the conjectured value of  $\frac{36221472}{936239725} \approx 0.0386882$ .)

Similarly, for the generic *nondegenerate* complex and real two-qubit states, we can achieve fits within 0.7% to *both* the conjectured HS separability probabilities of  $\frac{8}{33}$  and  $\frac{8}{17}$ , respectively, by taking in the real case the Euler-angle separability function to be  $I_{\left(1-VAD(\rho)\right)^2}(24, 28)$  (Fig. 22) and its square in the complex case. (Use of its fourth power to estimate the HS *quaternionic* two-qubit separability probability yielded a result 0.795969 as large as the value,  $\frac{72442944}{936239725} \approx 0.0795969$ , conjectured above (15).)

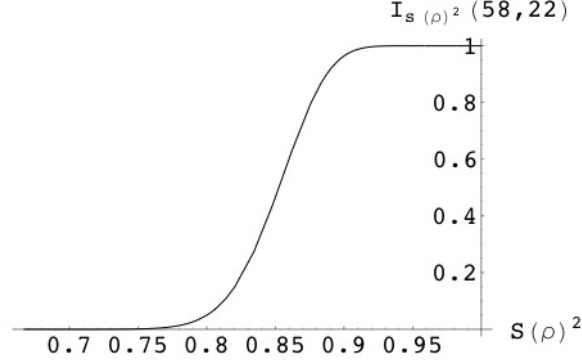


FIG. 21: Incomplete beta function estimate of the *bivariate* Euler-angle separability function that closely reproduces the conjectured Hilbert-Schmidt *minimally degenerate* two-qubit real, complex and quaternionic separability probabilities

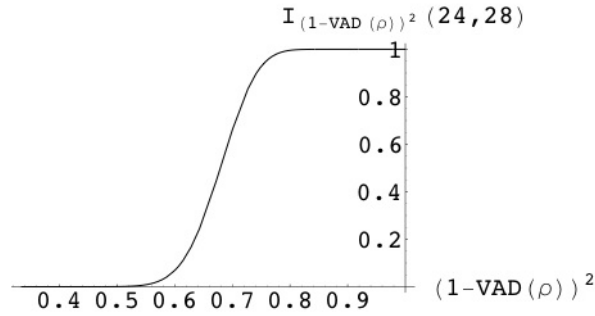


FIG. 22: Incomplete beta function estimate of the *trivariate* Euler-angle separability function that closely reproduces the conjectured Hilbert-Schmidt *nondegenerate* two-qubit real, complex and quaternionic separability probabilities

#### IV. SUMMARY

We have extended the findings and analyses of our two recent studies [11] and [17] by, first, obtaining numerical estimates of the separability function based on the (Euclidean, flat) Hilbert-Schmidt (HS) metric for the 27-dimensional convex set of quaternionic two-qubit systems (sec. II A). The estimated function closely conformed to our previously-formulated Dyson-index ( $\beta = 1, 2, 4$ ) ansatz, dictating that the quaternionic ( $\beta = 4$ ) separability function should be exactly proportional to the square of the separability function for the 15-dimensional convex set of two-qubit complex ( $\beta = 2$ ) systems, as well as the fourth power of the separability function for the 9-dimensional convex set of two-qubit real ( $\beta = 1$ ) systems.

In particular, these additional analyses led us specifically to aver that

$$\mathcal{S}_{quat}^{HS}(\mu) = \left(\frac{6}{71}\right)^2 \left((3 - \mu^2)\mu\right)^4 = (\mathcal{S}_{complex}^{HS}(\mu))^2, 0 \leq \mu \leq 1. \quad (69)$$

Here,  $\mu = \sqrt{\frac{\rho_{11}\rho_{44}}{\rho_{22}\rho_{33}}}$ , where  $\rho$  denotes a  $4 \times 4$  two-qubit density matrix. We have, thus, been able to supplement (*and* fortify) our previous assertion that the HS separability probability of the two-qubit complex states is  $\frac{8}{33} \approx 0.242424$ , claiming that its quaternionic counterpart is  $\frac{72442944}{936239725} \approx 0.0773765$ . We have also commented on and analyzed the odd  $\beta = 1$  and  $\beta = 3$  cases (sec. II B), which still remain somewhat problematical.

Further, we found (sec. II C) strong evidence of adherence to the Dyson-index ansatz for the 25-dimensional real and 35-dimensional complex qubit-*qutrit* systems with real HS separability function being proportional to a function of the form,  $1 - (1 - \nu_1\nu_2)^{\frac{5}{2}}$ , with  $\nu_1, \nu_2$  defined in (4). Subject to the validity of this separability function, we have obtained the corresponding  $R_2$  constants ( $\beta = 1, \dots, 4$ ) and estimated the complementary  $R_1$  constants (the products  $R_1R_2$  giving throughout, in our fundamental paradigm, the desired separability probabilities).

Then (sec. II D), we determined that in terms of the Bures (minimal monotone) metric—for certain, basic simple scenarios (in which the diagonal entries of  $\rho$  are unrestricted, and one or two off-diagonal [real, complex or quaternionic] pairs of entries are nonzero)—that the Dyson-index power relations no longer strictly hold, but come remarkably close to doing so.

Finally (sec. III), we examined the possibility of defining “separability functions” using the Euler-angle parameterization of Tilma, Byrd and Sudarshan [31], rather than the Bloore (correlation/off-diagonal scaling) framework [19]. Although now we are, *prima facie*, faced with a trivariate (in the complex two-qubit case) function, rather than a univariate one, we do not encounter the problem of having to determine an overall normalization factor for the separability function, since it is known that any density matrix with all eigenvalues equal to one another must be separable. It also appears that this simplifying feature further extends to the case where minimally degenerate (boundary) complex qubit-qubit states are considered (sec. III C), with any such state having its three non-zero eigenvalues all equal to  $\frac{1}{3}$  (lying on the boundary of the separable ball  $R(\rho) = 3$ ) being necessarily separable. Use of the estimated Euler-angle trivariate separability function lent still further (numerical) support to the  $\frac{8}{33}$  conjecture [17] for the HS separability probability (and the associated  $\frac{4}{33}$  conjecture for the hyperarea of the minimally degenerate two-qubit states) and the  $\frac{1680(\sqrt{2}-1)}{\pi^8}$

“silver mean” conjecture [8] for the Bures separability probability of generic complex two-qubit states.

### Acknowledgments

I would like to express appreciation to the Kavli Institute for Theoretical Physics (KITP) for computational support in this research. Also K, Życzkowski alerted me to the relevance of [69], and M. Trott assisted with certain computations.

- 
- [1] K. Życzkowski, P. Horodecki, A. Sanpera, and M. Lewenstein, *Phys. Rev. A* **58**, 883 (1998).
  - [2] J. E. Avron, G. Bisker, and O. Kenneth, *J. Math. Phys.* **48**, 102107 (2007).
  - [3] T. Tilma and E. C. G. Sudarshan, *J. Phys. A* **35**, 10467 (2002).
  - [4] P. B. Slater, *J. Phys. A* **32**, 8231 (1999).
  - [5] P. B. Slater, *J. Phys. A* **32**, 5261 (1999).
  - [6] P. B. Slater, *Euro. Phys. J. B* **17**, 471 (2000).
  - [7] P. B. Slater, *J. Opt. B* **2**, L19 (2000).
  - [8] P. B. Slater, *J. Geom. Phys.* **53**, 74 (2005).
  - [9] P. B. Slater, *Phys. Rev. A* **71**, 052319 (2005).
  - [10] P. B. Slater, *J. Phys. A* **39**, 913 (2006).
  - [11] P. B. Slater, *Phys. Rev. A* **75**, 032326 (2007).
  - [12] R. E. Kass, *Statist. Sci.* **4**, 188 (1989).
  - [13] K. Życzkowski and H.-J. Sommers, *J. Phys. A* **36**, 10115 (2003).
  - [14] H.-J. Sommers and K. Życzkowski, *J. Phys. A* **36**, 10083 (2003).
  - [15] M. L. Mehta, *Random Matrices* (Elsevier/Academic, Amsterdam, 2004).
  - [16] A. Andai, *J. Phys. A* **39**, 13641 (2006).
  - [17] P. B. Slater, *J. Phys. A* **40**, 14279 (2007).
  - [18] P. B. Slater, arXiv:0708.4208.
  - [19] F. J. Bloore, *J. Phys. A* **9**, 2059 (1976).
  - [20] H. Joe, *J. Multiv. Anal.* **97**, 2177 (2006).
  - [21] D. Kurowicka and R. Cooke, *Lin. Alg. Applics.* **372**, 225 (2003).

- [22] D. Kurowicka and R. M. Cooke, *Lin. Alg. Applics.* **418**, 188 (2006).
- [23] S. Guiasu, *Phys. Rev. A* **36**, 1971 (1987).
- [24] O. Gühne, P. Hyllus, O. Gittsovich, and J. Eisert, *Phys. Rev. Lett.* **99**, 130504 (2007).
- [25] V. E. Mkrtchian and V. O. Chaltykyan, *Opt. Commun.* **63**, 239 (1987).
- [26] A. Peres, *Phys. Rev. Lett.* **42**, 683 (1979).
- [27] S. L. Adler, *Quaternionic quantum mechanics and quantum fields* (Oxford, New York, 1995).
- [28] J. Batle, A. R. Plastino, M. Casas, and A. Plastino, *Opt. Spect.* **94**, 1562 (2003).
- [29] A. Peres, *Phys. Rev. Lett.* **77**, 1413 (1996).
- [30] M. Horodecki, P. Horodecki, and R. Horodecki, *Phys. Lett. A* **223**, 1 (1996).
- [31] T. Tilma, M. Byrd, and E. C. G. Sudarshan, *J. Phys. A* **35**, 10445 (2002).
- [32] A. K. Gupta and S. Nadarajah, *Handbook of Beta Distribution and Its Applications* (Marcel Dekker, New York, 2004).
- [33] F. J. Dyson, *Commun. Math. Phys.* **19**, 235 (1970).
- [34] P. B. Slater, [quant-ph/0602109](#).
- [35] R. Bellman, *Dynamic Programming* (Princeton Univ., Princeton, 1957).
- [36] F. Y. Kuo and I. H. Sloan, *Not. Amer. Math. Soc.* **52**, 1320 (2005).
- [37] G. Ökten, *MATHEMATICA in Educ. Res.* **8**, 52 (1999).
- [38] H. Faure and S. Tezuka, in *Monte Carlo and Quasi-Monte Carlo Methods 2000 (Hong Kong)*, edited by K. T. Tang, F. J. Hickernell, and H. Niederreiter (Springer, Berlin, 2002), p. 242.
- [39] L. Lovász and S. Vempala, *J. Comput. Syst. Sci* **72**, 392 (2006).
- [40] M. Dyer, A. Frieze, and R. Kannan, *J. ACM* **38**, 1 (1991).
- [41] P. B. Slater, *J. Math. Phys.* **37**, 2682 (1996).
- [42] T. Jiang, *J. Math. Phys* **46**, 052106 (2005).
- [43] J. Sánchez-Ruiz, *Phys. Rev. E* **52**, 5653 (1995).
- [44] S. Sen, *Phys. Rev. Lett.* **77**, 1 (1996).
- [45] F. R. Pfaff, *Amer. Math. Mon.* **107**, 156 (2000).
- [46] M. Budden, P. Hadavas, L. Hoffman, and C. Pretz, *Appl. Math. E-Notes* **7**, 53 (2007).
- [47] I. Bengtsson and K. Życzkowski, *Geometry of Quantum States* (Cambridge, Cambridge, 2006).
- [48] M. J. W. Hall, *Phys. Lett. A* **242**, 123 (1998).
- [49] P. B. Slater, *Phys. Lett. A.* **247**, 1 (1998).
- [50] M. Asorey, G. Sclarici, and L. Solombrino, *Phys. Rev. A* **76**, 012111 (2007).

- [51] J. B. Kogut, M. A. Stephanov, D. Toublan, J. J. M. Verbaarschot, and A. Zhitnitsky, Nucl. Phys. B **582**, 477 (2000).
- [52] M. Caselle and U. Magnea, Phys. Rep. **394**, 41 (2004).
- [53] J. Dittmann, J. Phys. A **32**, 2663 (1999).
- [54] M. Hübner, Phys. Lett. A **163**, 239 (1992).
- [55] J. Dittmann, Sem. Sophus Lie **3**, 73 (1993).
- [56] D. Bruß and C. Macchiavello, Found. Phys. **35**, 1921 (2005).
- [57] D. Collins, N. Gisin, N. Linden, S. Massar, and S. Popescu, Phys. Rev. Lett. **88**, 040404 (2002).
- [58] S. R. Finch, *Mathematical Constants* (Cambridge, New York, 2003).
- [59] H. N. V. Temperley and M. E. Fisher, Philos. J. **6**, 1061 (1961).
- [60] N. D. Gagunashvili and V. B. Priezzhev, Theor. Math. Phys. **39**, 347 (1979).
- [61] S. J. Akhtarshenas, arXiv:0705.1965.
- [62] S. Szarek, I. Bengtsson, and K. Życzkowski, J. Phys. A **39**, L119 (2006).
- [63] D. J. Gross, M. J. Perry, and L. G. Yaffe, Phys. Rev. D **25**, 330 (1982).
- [64] I. G. Macdonald, *Symmetric Functions and Hall Polynomial* (Oxford, New York, 1995).
- [65] A. O. Pittenger and M. H. Rubin, Lin. Alg. Applics. **346**, 47 (2002).
- [66] D. Petz and C. Sudár, J. Math. Phys. **37**, 2662 (1996).
- [67] J. Batle, M. Casas, A. Plastino, and A. R. Plastino, Phys. Lett. A **353**, 161 (2006).
- [68] J. Batle, A. R. Plastino, M. Casas, and A. Plastino, Phys. Lett. A **298**, 301 (2002).
- [69] F. Verstraete, K. Audenaert, and B. D. Moor, Phys. Rev. A **64**, 012316 (2001).
- [70] R. Hildebrand, Phys. Rev. A **76**, 052325 (2007).